The alteration history of the Jbilet Winselwan CM carbonaceous chondrite: An analog for Ctype asteroid sample return

Journal Item

The Meteoritical Society

Meteoritics & Planetary Science 1–23 (2018)
doi: 10.1111/maps.13224

The alteration history of the Jbilet Winselwan CM carbonaceous chondrite: An analog for C-type asteroid sample return

A. J. KING[1*], S. S. RUSSELL[1], P. F. SCHOFIELD[1], E. R. HUMPHREYS-WILLIAMS[2], S. STREKOPYTOV[2], F. A. J. ABERNETHY[3], A. B. VERCHOVSKY[3], and M. M. GRADY[3]

[1]Planetary Materials Group, Department of Earth Sciences, Natural History Museum, Cromwell Road, London SW7 5BD, UK
[2]Imaging and Analysis Centre, Natural History Museum, Cromwell Road, London SW7 5BD, UK
[3]Department of Physical Sciences, The Open University, Walton Hall, Milton Keynes MK7 6AA, UK
[*]Corresponding author. E-mail: a.king@nhm.ac.uk

(Received 23 December 2017; revision accepted 26 October 2018)

Abstract–Jbilet Winselwan is one of the largest CM carbonaceous chondrites available for study. Its light, major, and trace elemental compositions are within the range of other CM chondrites. Chondrules are surrounded by dusty rims and set within a matrix of phyllosilicates, oxides, and sulfides. Calcium- and aluminum-rich inclusions (CAIs) are present at ≤1 vol% and at least one contains melilite. Jbilet Winselwan is a breccia containing diverse lithologies that experienced varying degrees of aqueous alteration. In most lithologies, the chondrules and CAIs are partially altered and the metal abundance is low (<1 vol%), consistent with petrologic subtypes 2.7–2.4 on the Rubin et al. (2007) scale. However, chondrules and CAIs in some lithologies are completely altered suggesting more extensive hydration to petrologic subtypes ≤2.3. Following hydration, some lithologies suffered thermal metamorphism at 400–500 °C. Bulk X-ray diffraction shows that Jbilet Winselwan consists of a highly disordered and/or very fine-grained phase (73 vol%), which we infer was originally phyllosilicates prior to dehydration during a thermal metamorphic event(s). Some aliquots of Jbilet Winselwan also show significant depletions in volatile elements such as He and Cd. The heating was probably short-lived and caused by impacts. Jbilet Winselwan samples a mixture of hydrated and dehydrated materials from a primitive water-rich asteroid. It may therefore be a good analog for the types of materials that will be encountered by the Hayabusa-2 and OSIRIS-REx asteroid sample-return missions.

INTRODUCTION

The Jbilet Winselwan meteorite was found on May 24, 2013 near Smara in Western Sahara. It consists of numerous stones ranging from a few grams up to ~900 g, with a total recovered mass of ~6 kg. The entry in the Meteoritical Bulletin describes Jbilet Winselwan as containing chondrules, chondrule pseudomorphs, and a few calcium-aluminum-rich inclusions (CAIs) set within a dark, fine-grained matrix (Ruzicka et al. 2015). Analysis by X-ray diffraction (XRD) identified serpentine, smectite, and tochilinite ($Fe_{5-6}[Mg, Fe]_5S_6[OH]_{10}$). The oxygen isotopic compositions of two pieces of Jbilet Winselwan were reported as $\delta^{18}O = 3.811 \pm 0.09$ and 5.851 ± 0.016, $\delta^{17}O = -2.446 \pm 0.040$ and -0.601 ± 0.026, which in combination with the petrography led to its classification as a CM ("Mighei-type") carbonaceous chondrite (Ruzicka et al. 2015). The CM carbonaceous chondrites typically contain ~10 wt% extraterrestrial H_2O locked-up in abundant (~70 vol%) phyllosilicates and are interpreted as the products of low temperature (<150 °C) aqueous alteration on primitive asteroid parent bodies (e.g., Brearley 2006).

There are >500 recognized CM chondrites (~1% of all known meteorites), of which 16 are falls and ~90% are finds from Antarctica. Jbilet Winselwan is currently the fourth largest CM chondrite (behind the falls Murchison, Murray, and Mighei), and one of only ~50 samples recovered from a hot desert environment. The

residence time of meteorites in hot deserts is expected to be significantly shorter than those found in Antarctica (Bland et al. 2006). Fragments of Jbilet Winselwan are wind ablated and have cracks filled with secondary alteration products but it otherwise has a low weathering grade of W1 (Ruzicka et al. 2015). As a large and relatively fresh example of a CM chondrite, Jbilet Winselwan is being widely used in studies by the meteorite community (e.g., Göpel et al. 2015; Van Kooten et al. 2016; Thangjam et al. 2016; Chan et al. 2017; Friend et al. 2018).

Initial observations of Jbilet Winselwan by ourselves and other research groups highlighted wide variations in the degree of aqueous alteration and led to suggestions that it is an impact breccia (Russell et al. 2014; Pernet-Fisher et al. 2014; Zolensky et al. 2016; Friend et al. 2018). It was also proposed that Jbilet Winselwan belongs to a group of CM chondrites, now comprising of >20 meteorites, that following aqueous alteration suffered thermal metamorphism (Russell et al. 2014; Grady et al. 2014; Zolensky et al. 2016). Evidence for heating after the aqueous alteration includes the presence of a dehydrated phyllosilicate phase, fine-grained, recrystallized olivine in the matrix, and melted Fe-sulfide masses (e.g., Nakamura 2005). However, the mechanism, timing, and duration of the metamorphic event(s) that produced the heated CM chondrites remains poorly constrained. Detailed investigation of these samples is also timely given that many low albedo C-type asteroids—including Ryugu, the target for the Hayabusa-2 sample-return mission—have surface spectra consistent with mixtures of both hydrated and dehydrated CM materials (Hiroi et al. 1993, 1996; Vilas 2008).

Here, we have undertaken a collaborative effort to study the Jbilet Winselwan specimen (BM2013, M4) acquired in 2013 by the Natural History Museum (NHM), London, UK. The micro- and bulk-scale properties of the Jbilet Winselwan meteorite have been characterized using a combination of scanning electron microscopy (SEM); electron microprobe analysis (EMPA); XRD; thermogravimetric analysis (TGA); infrared (IR) spectroscopy; and light, major, and trace element analysis. Our aim was to establish the alteration history of Jbilet Winselwan and determine its relationship with other hydrated and dehydrated CM chondrites, and potential asteroid parent bodies.

SAMPLES AND METHODS

SEM/EMPA

Four polished thin sections and one polished probe mount were prepared from a single chip (0.57 g, JW-1) of Jbilet Winselwan. The size of the sections ranges from ~10 mm^2 to 23 mm^2. For each sample, backscattered electron (BSE) images and energy-dispersive X-ray (EDS) element maps were acquired using a Zeiss EVO 15LS SEM equipped with an Oxford Instruments X-Max80 EDS silicon drift detector (SSD) in the Imaging and Analysis Centre (IAC) at the NHM. Analyses were carried out at 20 kV with a beam current of 3 nA and the EDS system was calibrated using cobalt metal. Mineral compositions were determined in one section (JW-1-A) and the probe mount (JW-1-E) using a Cameca SX100 electron microprobe and wavelength-dispersive X-ray spectroscopy (WDS) in the IAC at the NHM. Spot analyses were made on chondrule olivines and the matrix using a 1 μm beam at 15 kV and 20 nA. Standards included Na (jadeite), Mg (forsterite—synthetic), Al (corundum—synthetic), Si (wollastonite), P (scandium phosphate), S (barite and ZnS), K (potassium bromide), Ca (wollastonite), Ti (rutile—synthetic), Cr (chromium oxide), Mn (manganese titanium oxide), Fe (fayalite), and Ni (nickel oxide [II]). The detection limits for all elements were <500 ppm and the analytical errors were ~0.1 wt% for most elements.

PSD-XRD

Two separate ~50 mg chips free of fusion crust (JW-2 and JW-3) were powdered to a grain size of <35 μm, immediately packed into aluminum sample wells, and analyzed using an INEL X-ray diffractometer equipped with a curved 120° position sensitive detector (PSD) at the NHM. Copper $K_{\alpha 1}$ radiation was selected with a Ge 111 monochromater and the size of the beam on the sample was restricted to 0.24 mm × 2 mm using post-monochromator slits. XRD patterns were collected from the Jbilet Winselwan samples for 16 h and from pure standards of minerals present in the meteorite for 30 min.

Phase quantification was achieved using a profile-stripping method that has been applied to >50 carbonaceous chondrites in our laboratory (Bland et al. 2004; Howard et al. 2009, 2010, 2011, 2015; King et al. 2015a, 2017). The method involved scaling the XRD pattern of a mineral standard and then reducing its intensity by a factor to match its intensity in the XRD pattern of the meteorite sample. At this point, the standard pattern was subtracted to leave a residual meteorite pattern. This process was repeated for all phases identified in the meteorite until there were zero counts left in the residual. The fit factors for the mineral standards were then corrected for relative differences in X-ray absorption to give a final volume fraction in the meteorite (Cressey and Schofield 1996). Modal abundances are limited to phases present at ≥1 vol% and the uncertainties are <5% (King et al. 2015a).

TGA

Approximately 12 mg of JW-2 and 16 mg of JW-3 were analyzed using a TA Instruments SDT Q600 TGA at the NHM. For comparison with other CM chondrites, and to monitor the reproducibility of our measurements, we also analyzed seven aliquots (~10 mg each) of the Murchison (CM2) meteorite. Each sample was loaded into an alumina crucible and analyzed under an N_2 flow of 100 ml min^{-1}. The mass loss from the samples was recorded as they were heated from 25 to 1000 °C at 10 °C min^{-1}. The sensitivity of the TGA balance is 0.1 μg and the overall error on the measured mass loss fractions is ~0.1%.

The resulting DTG (wt%/°C) curve shows how the rate of mass loss changes during heating, with the peak positions as a function of temperature often characteristic of mineral groups and individual phases. In general, previous studies of aqueously altered carbonaceous chondrites have shown that terrestrial adsorbed water is removed at temperatures of <200 °C, water from Fe-(oxy)hydroxides is released between 200–400 °C, dehydration and dehydroxylation of phyllosilicates occurs at 400–770 °C, and from 770–900 °C CO_2 is produced by the breakdown of carbonate minerals (Garenne et al. 2014; King et al. 2015b).

IR Spectroscopy

A ~3 mg aliquot of JW-2 was mixed with 300 mg of KBr and compressed to form a 13 mm diameter pellet. In addition, we also prepared pellets of the CM2 chondrite falls Murchison and Santa Cruz, which were studied during the same analytical session. Transmission mid-IR spectra (2–25 μm) were obtained from the pellets under a low vacuum using an offline benchtop Bruker Vertex 80V FTIR interferometer at beamline B22 at Diamond Light Source, UK. Because the pellets were stored and analyzed at room temperature, the 3 μm feature—attributed to -OH/H_2O in phyllosilicates and Fe-(oxy)hydroxides—was likely affected by absorbed terrestrial water (e.g., Beck et al. 2010, 2014a). Instead, we focus here on the 5–25 μm region of the spectra.

Major and Trace Element Analysis

The major and trace element composition of Jbilet Winselwan was determined using inductively coupled plasma optical emission spectroscopy (ICP-OES) and inductively coupled plasma mass spectrometry (ICP-MS) in the IAC at the NHM. For comparison, we also determined the major element abundances in a sample of the aqueously altered and thermally metamorphosed CM chondrite EET 96029 (Lee et al. 2016) using the same analytical procedure described below.

A chip of Jbilet Winselwan (49.4 mg, JW-4) was powdered in a clean laboratory using an agate mortar and pestle. Approximately 40 mg of the powder was pretreated with 1 mL of concentrated HNO_3 and fused with 120 mg of $LiBO_2$ in a Pt/Au crucible. The resulting flux was dissolved in 0.64M HNO_3 before major element abundances were determined in triplicate using a Thermo iCap 6500 Duo ICP-OES instrument. The instrument was calibrated using a range of certified reference materials (CRMs), which were prepared in the same way. The standards DTS-2B (dunite) and JB-1 (basalt) were analyzed as unknown samples to provide quality control.

Trace element abundances were determined in a separate powdered chip of Jbilet Winselwan (72 mg, JW-5). Approximately 23 mg of the powder was digested in HF + $HClO_4$ + HNO_3 before analysis in duplicate using an Agilent 7700x ICP-MS instrument. Nonisobaric interferences were reduced by tuning CeO^+/Ce^+ and Ba^{++}/Ba^+ to <1%; for Eu, Gd, Tb, Hf, Ta, and W, corrections were applied for polyatomic interferences from Ba, Ce+Pr, Nd, Dy, Ho, and Er, respectively (Strekopytov and Dubinin 1997; Ferrat et al. 2012). The accuracy of the trace element analyses was monitored using the CRMs BCR-2 (basalt), JLs-1 (limestone), and SY-2 (syenite).

C, N, and Noble Gas Analysis

The abundances and isotopic compositions of C, N, and He were determined using a custom-built high-sensitivity stepped combustion mass spectrometer ("Finesse") at the Open University, UK. Briefly, an uncrushed ~5 mg chip of Jbilet Winselwan (JW-6) was weighed into a platinum foil and heated under pure oxygen for ~40 min in 100 °C increments from room temperature to 1400 °C. The resulting CO_2, N_2, and He gases were then cryogenically separated from other by-products (e.g., SO_2, H_2O, etc.) of the combustion before being collected in three static-mode mass spectrometers (one each for carbon, nitrogen, and helium). The data were corrected for system blanks (typically <10 ng for carbon, <1 ng for nitrogen, and $<1 \times 10^{-7}$ mL g^{-1} for He) determined by analyzing an empty clean platinum foil using the same procedure (see Mortimer et al. 2016).

RESULTS

Microscale Properties

Petrography and Mineral Compositions

Each of the thin sections show very pristine chondrules composed of primary olivine embedded in a

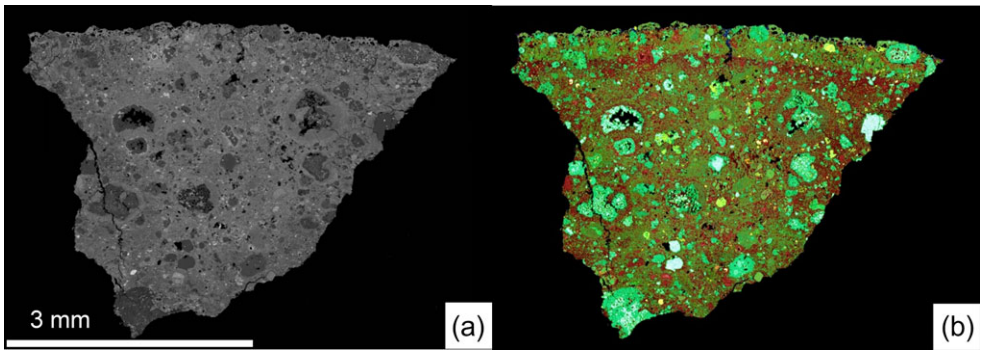

Fig. 1. BSE image (a) and EDS Element map (b) of Jbilet Winselwan (JW-1-B). Si = blue, Mg = green, Fe = red, Ca = yellow, Al = white. Note that fusion crust can be seen along the top of the section.

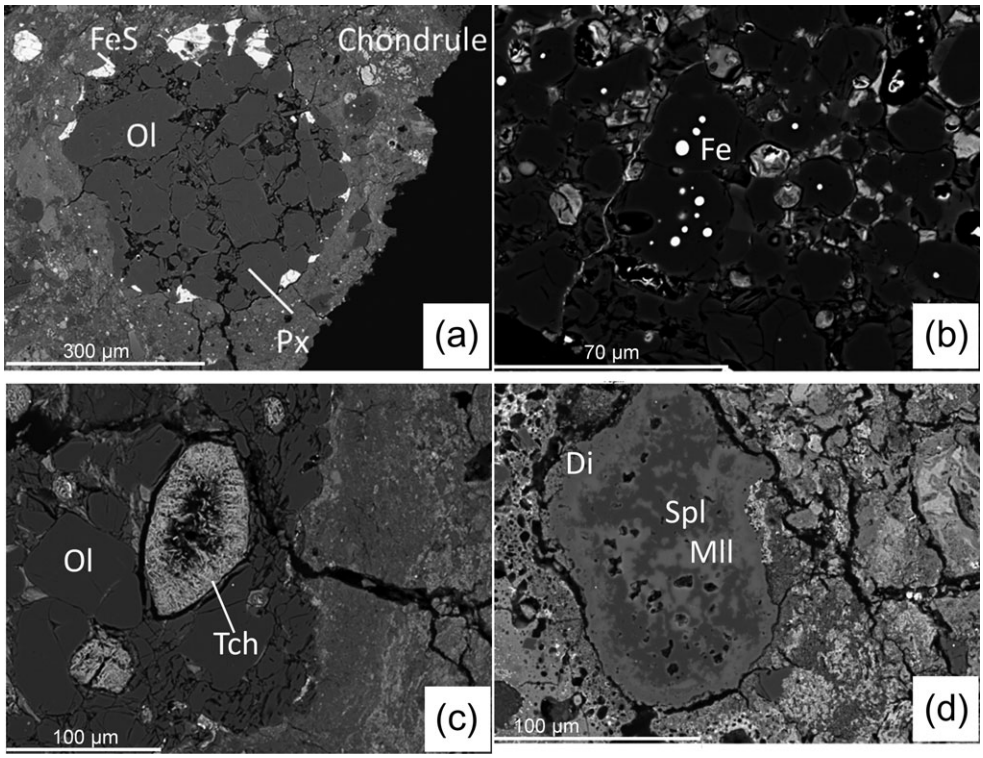

Fig. 2. BSE images of mildly altered portions of Jbilet Winselwan (JW-1-A). a) Forsteritic porphyritic chondrule, (b) forsteritic chondrules with metal blebs, (c) large tochilinite mass that likely replaced metal within a chondrule, and (d) compact type A CAI (JW-CAI-1). Ol = olivine, Px = pyroxene, Di = diopside, Spl = spinel, Mll = melilite, Fe = metal, Tch = tochilinite.

fine-grained phyllosilicate matrix (Fig. 1). The chondrule/matrix ratio determined from point counting is ~50:50. The chondrules show no signs of deformation and are surrounded by dusty rims (50–100 µm thick). The range of compositions for type I chondrules is $Fo_{91–100}$ and for type II chondrules is $Fo_{66–77}$. Chondrules often contain minor pyroxene that is more abundant toward the rim (Fig. 2a). Nearly all the chondrules are porphyritic in texture, and the type I chondrules often contain blebs of metal (Fig. 2b), consistent with moderate aqueous alteration (Rubin et al. 2007). Tochilinite is observed in some chondrules (Fig. 2c).

CAIs are relatively small (<500 µm) in size and present (from point counting) at levels of ≤1 vol%. Spinel-pyroxene CAIs are the most common type observed, often showing little alteration of the diopside. One rounded, compact CAI, JW-CAI-1, is ~150 mm in maximum dimension and composed of melilite and spinel surrounded by a thick diopside rim (Fig. 2d). This CAI does not exhibit any observable secondary mineralization.

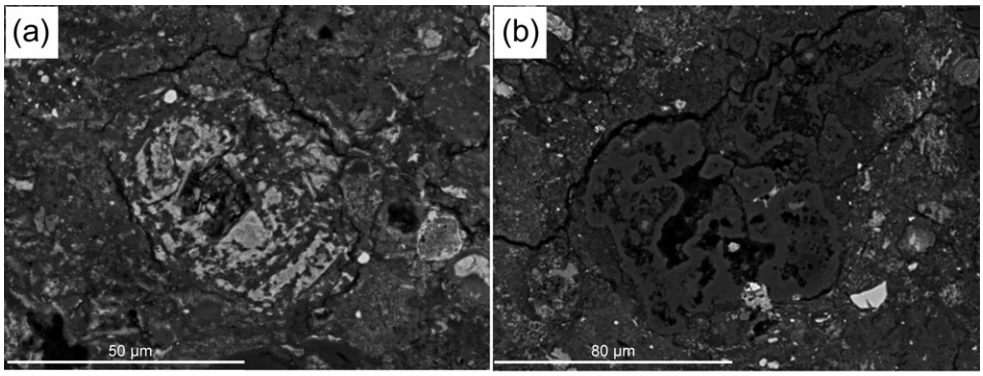

Fig. 3. BSE images of a highly altered chondrule (a) and CAI (b) in Jbilet Winselwan (JW-1-E).

Table 1. Elemental composition (wt%) of Jbilet Winselwan matrix measured by EMPA in thin sections JW-1-A and JW-1-E. *n* is the number of spot analyses and values in parentheses are 1 standard deviation.

	JW-1-A	JW-1-E
SiO_2	26.0 (3.9)	27.5 (3.3)
TiO_2	0.1 (0.2)	0.1 (0.03)
Al_2O_3	2.8 (2.2)	2.5 (0.4)
FeO	32.4 (5.5)	32.8 (4.2)
NiO	2.0 (0.6)	1.7 (0.5)
Cr_2O_3	0.4 (0.1)	0.4 (0.1)
MnO	0.2 (0.05)	0.2 (0.1)
MgO	13.4 (3.4)	13.7 (2.9)
CaO	1.7 (1.0)	1.7 (0.7)
Na_2O	0.8 (0.2)	0.7 (0.2)
K_2O	0.1 (0.04)	0.2 (0.1)
S	1.9 (0.8)	1.9 (0.8)
P_2O_5	0.4 (0.3)	0.2 (0.2)
Total	82.3 (4.0)	83.5 (3.1)
n	58	73
MgO/FeO	0.41	0.42
S/SiO_2	0.07	0.07

The probe mount of Jiblet Winselwan (JW-1-E) shows much more extensive aqueous alteration than the other sections. Although chondrules are visible in this sample, they are extensively altered, with most showing total replacement of the primary phenocryst phases by phyllosilicates (Fig. 3a). Likewise, in this sample CAIs are present but heavily altered, with often only the sinuous diopside rim remaining and surrounded by a mixture of fine-grained Na-Fe-rich alteration products (Fig. 3b).

EMPA of the matrix gives a mean total of 82.3 (±4.0 wt%) in JW-1-A and 83.5 (±3.1) wt% in JW-1-E (Table 1). The low totals are consistent with the presence of -OH/H_2O-bearing minerals, as well as other factors such as pores and variable mineral densities. The elemental composition of the matrix is similar to serpentine and in agreement with other CM chondrites (Fig. 4).

Bulk Properties

Modal Mineral Abundances

Figure 5 shows an XRD pattern for Jbilet Winselwan (JW-3) compared to the CM2 chondrite fall Santa Cruz, which experienced moderate aqueous alteration and no significant thermal metamorphism. The crystalline phases identified in Jbilet Winselwan are olivine, enstatite, magnetite, sulfides (pyrrhotite/troilite and pentlandite), and sulfates (gypsum and anhydrite). However, unlike other CM chondrites analyzed using PSD-XRD, we do not observe the diffraction peaks at ~12° and ~25°, and ~19° and ~61°, which are attributed to Fe- and Mg-rich phyllosilicates, respectively (Howard et al. 2009, 2011; King et al. 2017).

The modal mineralogy of Jbilet Winselwan is given in Table 2. There is little difference (<2 vol%) between the two samples analyzed (JW-2 and JW-3) and the average mineralogy is ~16 vol% olivine, ~6 vol% enstatite, ~1 vol% magnetite, ~3 vol% sulfides, and ~1 vol% sulfates. For both samples, following subtraction of the crystalline phases, we were left with a residual pattern greater than zero, while the sum of the fit factors was less than one. This indicates that Jbilet Winselwan contains a significant noncrystalline component. We cannot rule out the occurrence of amorphous silicates or poorly crystalline Fe-(oxy)hydroxides and rusts, but found that the residual patterns were in good agreement with the overall shape and intensity (when scaled) of our phyllosilicate standards excluding the diffraction peaks. Dehydration and dehydroxylation of phyllosilicates causes the loss of interlayer H_2O and structural -OH, and the formation of a highly disordered and/or very fine-grained phase. A lack of coherent diffraction from phyllosilicates is a common feature of heated CM chondrites when analyzed by XRD (Nakamura 2005; Tonui et al. 2014; King et al.

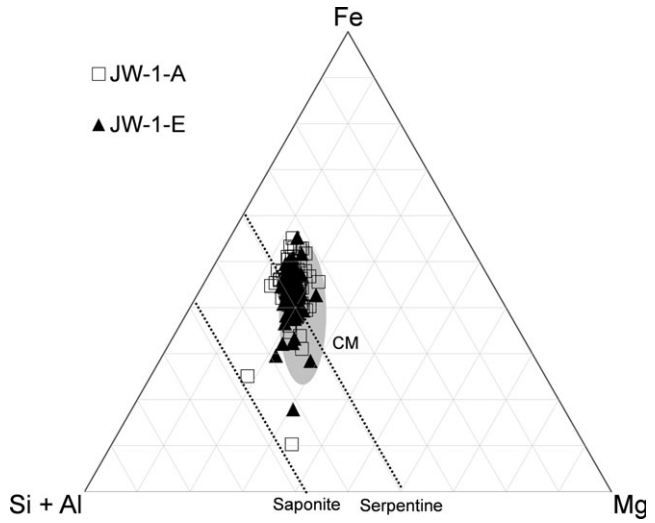

Fig. 4. Ternary diagram (element wt%) showing the composition of the matrix in Jbilet Winselwan thin sections JW-1-A and JW-1-E compared to CM chondrite matrix (gray ellipse, data from Zolensky et al. 1993).

2015a). We therefore attribute the remaining counts in the residual to a highly disordered and/or very fine-grained phase present at ~73 vol%, which we infer was originally phyllosilicates prior to dehydration during a thermal metamorphic event(s).

Abundance of Water/OH

Figure 6 shows the mass loss and DTG curves for the Jbilet Winselwan samples (JW-2 and JW-3). The curves are broadly similar and summarized in Table 3. Mass loss at temperatures of <200 °C is attributed to terrestrial alteration—the removal of adsorbed water (~50 °C) and the breakdown of sulfate minerals (~120 °C)—and is not considered further (Garenne et al. 2014; King et al. 2015b). In the regime where water is released from Fe-(oxy)hydroxides (200–400 °C), there is little mass loss for either JW-2 (2.0 wt%) or JW-3 (2.3 wt%). For both samples, this trend continues until there are two significant mass loss events at ~650 °C and ~750 °C. Overall, the total mass loss from 400–770 °C (where water is released from phyllosilicates) is 6.8 wt% for JW-2 and 8.2 wt% for JW-3. The variation in mass loss between 400 and 770 °C for seven aliquots of the Murchison meteorite was <1% (Table 3). The Jbilet Winselwan samples then lose little mass (1.6 wt% for JW-2 and 1.3 wt% for JW-3) in the region where carbonates are expected to break down (770–900 °C). Assuming that all of the mass loss between 200 and 770 °C is due to dehydration and dehydroxylation of Fe-(oxy)hydroxides and phyllosilicates (Garenne et al. 2014; King et al. 2015b), we estimate a H_2O abundance of 8.8 wt% for JW-2 and 10.5 wt% for JW-3.

Mid-IR Features

Figure 7 shows the mid-IR spectra from Jbilet Winselwan (JW-2), and the CM2 chondrites Murchison and Santa Cruz. Also included are spectra for cronstedtite, saponite, and San Carlos olivine standards collected under the same analytical conditions. The main component for each meteorite is a peak at ~10 μm and a broad feature at ~22 μm. These result from Si-O stretching and bending modes in the abundant phyllosilicates present within these meteorites. For all three meteorites, the position of the 10 μm feature best matches saponite rather than cronstedtite, in agreement with the observations of CM and CI chondrites by Beck et al. (2014a).

Jbilet Winselwan shows a distinct peak at ~11.2 μm, which is only a broad shoulder for Murchison and Santa Cruz. The position of this peak is consistent with olivine, and the intensity relative to the 10 μm feature suggests that the abundance is highest in Jbilet Winselwan (e.g., Beck et al. 2014a). This is further supported by the detection of a second olivine peak at ~16.3 μm in Jbilet Winselwan but not Murchison or Santa Cruz. A feature at ~7 μm from calcite is observed for Santa Cruz, but is not obviously present for either Jbilet Winselwan or Murchison. Jbilet Winselwan differs from the other meteorites with peaks at ~8.6, ~8.9, ~14.8, and ~16.8 that are from gypsum.

Major and Trace Element Composition

The bulk major element composition of Jbilet Winselwan is given in Table 4. Also provided are the compositions for two of the least altered CM chondrites, EET 96029 and Paris, and two CM chondrite falls, Maribo and Murchison. For most of the major elements, the composition of Jbilet Winselwan is consistent with other CM chondrites. The exception is CaO, which at 4.79 wt% is almost a factor of 3 higher than the typical values for CM chondrites.

The trace element composition of Jbilet Winselwan is given in Table 5. The rare earth element (REE) pattern for the fragment of Jbilet Winselwan analyzed in this study is distinct from other CM chondrites, with noticeable enrichments in Ho (×1.7), Er (×2.4), and Lu (×3.0) (Fig. 8a). Enrichments (×1.5–5.0) above typical CM chondrite abundances are also observed for Zr, Hf, Y, Th, U, Ta, Sr, Ba, and Li, while elements such as Cs, Tl, and Cd are depleted (by ~×3.0) (Fig. 8b).

Carbon and Nitrogen

Jbilet Winselwan contains 1.99 wt% carbon with a total $\delta^{13}C$ value of −6.5‰, and 917 ppm nitrogen with a total $\delta^{15}N$ value of +36.5‰ (Table 6). Stepped combustion profiles show that ~75% of the total carbon

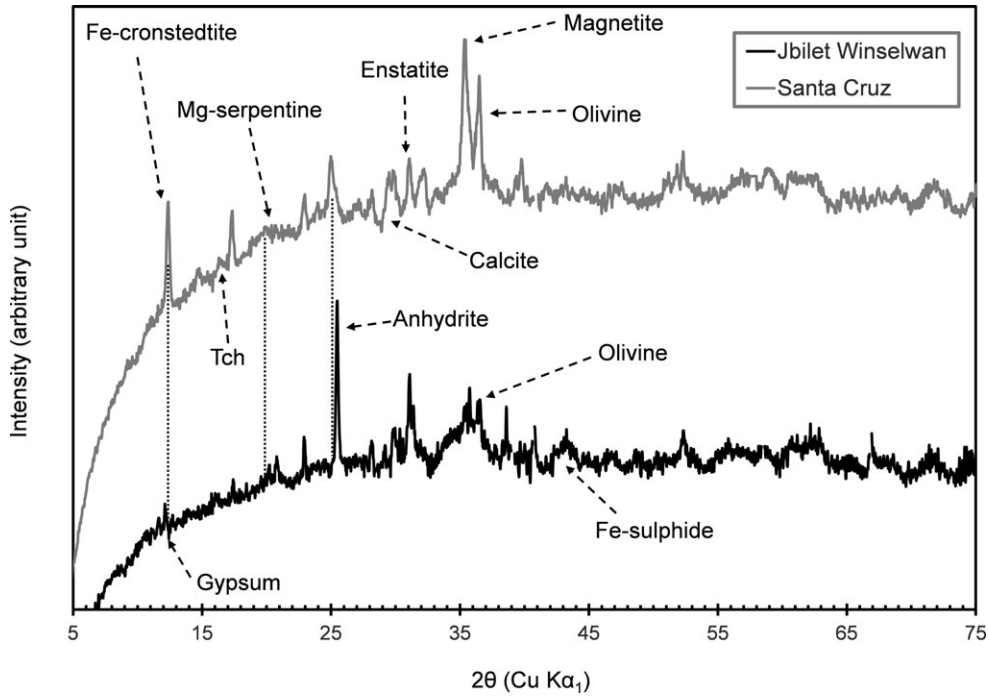

Fig. 5. PSD-XRD pattern for Jbilet Winselwan (JW-3) and CM2 chondrite Santa Cruz. Thermal metamorphism results in dehydration and dehydroxylation of phyllosilicates, causing the collapse of the phyllosilicate structure and hence a lack of coherent diffraction. Diffraction peaks from Fe- and Mg-rich phyllosilicates (~12° and ~25°, and ~19° and ~61°, respectively) are not observed for Jbilet Winselwan but are clearly identified in the XRD pattern of the unheated Santa Cruz. From the PSD-XRD analysis, the modal mineralogy of Santa Cruz is ~71 vol% phyllosilicate, ~16 vol% olivine, ~4 vol% enstatite, ~3 vol% magnetite, ~4 vol% Fe-sulfides, and ~2 vol% calcite. Tch = tochilinite.

Table 2. Modal mineralogy of Jbilet Winselwan. Approximately 50 mg of two different samples (JW-2 and JW-3) were analyzed by PSD-XRD. Jbilet Winselwan contains a highly disordered and/or very fine-grained phase, which we infer was phyllosilicates prior to dehydration during a thermal metamorphic event(s). The mass absorption coefficient for this phase was calculated from the phyllosilicate composition determined by EMPA. We conservatively estimate the uncertainties as 2–4% for crystalline phases and 3–5% for poorly crystalline materials (see King et al. [2015a] for details). The phyllosilicate fraction (PSF = total phyllosilicate abundance/[total anhydrous silicate + total phyllosilicate abundance]) is used to define the petrologic type in the Howard et al. (2015) classification scheme.

	Dehydrated phyllosilicates (vol%)	Olivine (vol%)	Enstatite (vol%)	Magnetite (vol%)	Sulfides (vol%)	Sulfates (vol%)	PSF	PSF classification
Jbilet Winselwan—2	72.2	16.6	5.1	1.1	3.7	1.3	0.77	1.5
Jbilet Winselwan—3	74.3	14.7	6.4	1.2	2.2	1.2	0.78	1.5
Average	73.3 (1.5)	15.7 (1.3)	5.8 (0.9)	1.2 (0.1)	3.0 (1.0)	1.3 (0.2)	0.78	1.5

and nitrogen combusted below 600 °C and ~99% below 800 °C (Fig. 9).

Combustion of carbon and nitrogen with variable isotopic compositions and C/N ratios below 800 °C suggests that Jbilet Winselwan contains multiple carbon- and nitrogen-bearing components, presumably mainly organic in nature. From 200–400 °C, the C/N ratio increased from ~33 to a maximum of ~87, coinciding with an increase in $\delta^{13}C$ from −11.5‰ to −2.1‰. At the same time, the $\delta^{15}N$ also increased from −6.3‰ to +23.5‰. Between 400 and 600 °C, the C/N ratio fell to ~14, while the $\delta^{13}C$ dropped to −8.8‰ and $\delta^{15}N$ increased to a maximum at 600 °C of +41.5‰. Combustion from 600 to 800 °C resulted in a second peak in the C/N ratio of ~57 at 800 °C, and decreases in the $\delta^{13}C$ and $\delta^{15}N$ values to −12.5‰ and +35.8‰, respectively. Above 800 °C, the C/N ratio fell to ~12, with $\delta^{13}C$ rising to a maximum of +262.9‰ at 1200 °C, and $\delta^{15}N$ to a minimum of −20.5‰ at 1100 °C. The isotope values are consistent with interpretation as being from combustion of presolar

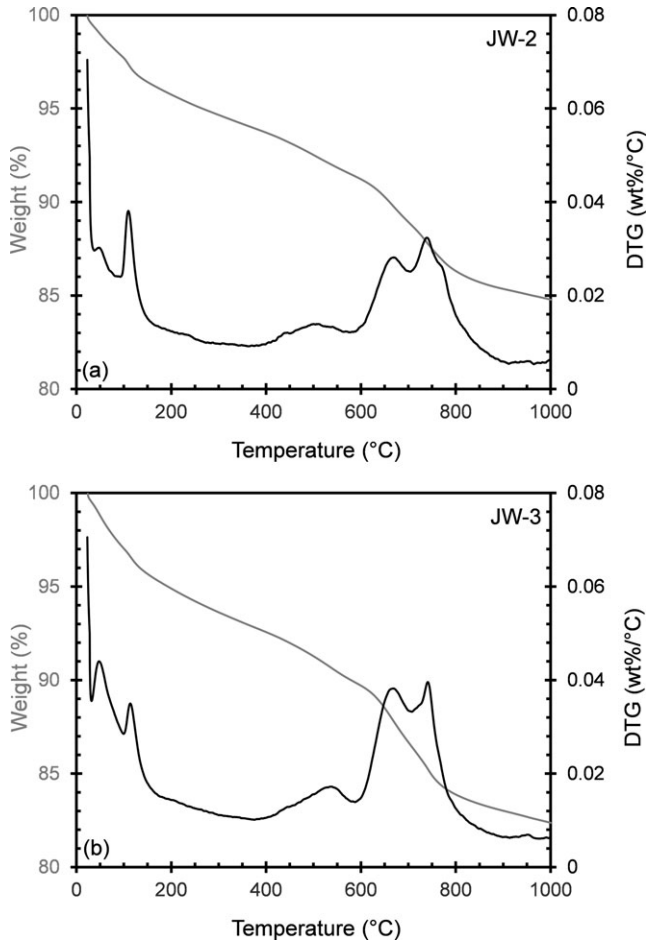

Fig. 6. Mass loss (gray) and DTG (black) curves for Jbilet Winselwan samples (a) JW-2 and (b) JW-3. The DTG curves are divided into different temperature regions related to the dehydration of terrestrial adsorbed H_2O and sulfates (25–200 °C), the dehydration and dehydroxylation of Fe-(oxy) hydroxides (200–400 °C) and phyllosilicates (400–770 °C), and the breakdown of carbonates (770–900 °C).

silicon carbide grains, as is characteristic of other carbonaceous chondrites. During the final combustion step at 1400 °C (<0.05% of total carbon and nitrogen), the $\delta^{13}C$ decreased to a minimum of −17.1‰, whereas the $\delta^{15}N$ increased to +16.5‰.

DISCUSSION

Classification

Based on mineralogy, petrography, and isotopic compositions, the initial studies of Jbilet Winselwan classified it as a CM chondrite (Russell et al. 2014; Pernet-Fisher et al. 2014; Ruzicka et al. 2015; Zolensky et al. 2016; Friend et al. 2018). We find that Jbilet Winselwan contains chondrules (Type I and II), CAIs, and isolated fragments often surrounded by dusty rims and set within a fine-grained matrix of phyllosilicates, oxides, and sulfides. The presence of a highly disordered phase, which we interpret as the thermal breakdown product of phyllosilicates, is consistent with the classification of Jbilet Winselwan as a CM chondrite. In addition, the bulk major and trace element composition of Jbilet Winselwan is generally in agreement with the CM chondrites, although there are some discrepancies (see the Terrestrial Weathering and REE Enrichments sections). Stepped combustion profiles for carbon and nitrogen in Jbilet Winselwan are similar to other reported CM chondrites, and Fig. 10 shows that the overall carbon and nitrogen abundances fall within the CM range.

Our observations show that Jbilet Winselwan is a breccia containing lithologies that record variable aqueous alteration and thermal metamorphism on the asteroid parent body, and since arriving on Earth has suffered some terrestrial weathering. In the following sections, we describe the effects of each of these processes on the Jbilet Winselwan meteorite. However, unraveling the alteration history of a complex, heterogeneous meteorite such as Jbilet Winselwan is challenging and we caution that analyses of different aliquots using multiple techniques sampling different volumes of material can result in discrepancies between data sets.

Terrestrial Weathering

The majority (~90%) of CM chondrites are finds from Antarctica, but in recent years there has been an increasing number retrieved from hot deserts, providing a new opportunity to discriminate between the effects of pre-terrestrial (i.e., parent body) and terrestrial alteration processes. The residence time of meteorites in hot desert environments is 15,000–20,000 yr, considerably shorter than the 10^5 yr for meteorites in Antarctica (Bland et al. 2006). In a hot desert, a meteorite quickly suffers physical and chemical weathering due to burial in soils and wind-blown dust; exposure to an oxidizing atmosphere; daytime temperatures >35 °C; and rare, although often significant, precipitation (e.g., Stelzner et al. 1999; Crozaz and Wadhwa 2001; Bland et al. 2006). There have been a number of studies investigating the effects of hot desert weathering on ordinary chondrites and achondrites (Barrat et al. 1999, 2001, 2003; Stelzner et al. 1999; Crozaz and Wadhwa 2001; Crozaz et al. 2003; Hezel et al. 2011), but few looking at carbonaceous chondrites. Jbilet Winselwan is therefore a potentially valuable meteorite for understanding the weathering of carbonaceous chondrites in hot deserts.

The Jbilet Winselwan meteorite was found in 2013 near the city of Smara in Western Sahara. Described as having a fresh fusion crust and some wind ablated

Table 3. Mass loss (wt%) as a function of temperature during TGA for two Jbilet Winselwan samples (JW-2 and JW-3). Mass loss occurs between 25 and 900 °C, and the DTG curves are divided into different temperature regions related to the dehydration of terrestrial adsorbed H_2O (25–200 °C), the dehydration and dehydroxylation of Fe-(oxy)hydroxides (200–400 °C) and phyllosilicates (400–770 °C), and the breakdown of carbonates (770–900 °C).

	Total mass loss (25–1000 °C)	25–200 °C	200–400 °C	400–770 °C	770–900 °C	H_2O (200–770 °C)	H (wt%)
Jbilet Winselwan—2	15.5	4.0	2.0	6.8	1.6	8.8	1.0
Jbilet Winselwan—3	17.5	4.9	2.3	8.2	1.3	10.5	1.2
Average	16.5 (1.4)	4.5 (0.6)	2.2 (0.2)	7.5 (1.0)	1.5 (0.2)	9.7 (1.2)	1.1 (0.1)
Murchison (n = 7)[a]		4.2 (0.2)	4.0 (0.2)	6.9 (0.5)	1.1 (0.1)	10.9 (0.4)	1.2 (0.1)
Murchison[b]		2.7	3.5	7.3	1.9	10.8	1.2

[a]Average values from seven aliquots; the standard deviation is given in brackets.
[b]Values taken from Garenne et al. (2014).

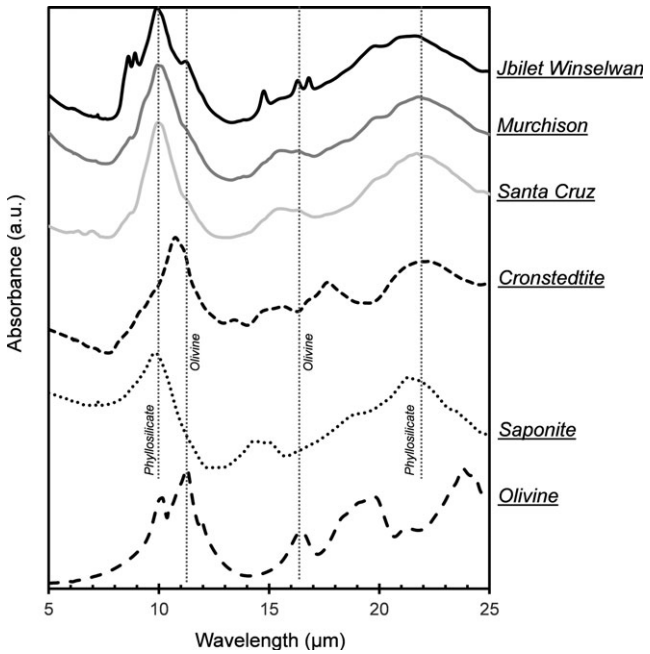

Fig. 7. Mid-IR spectra for the CM chondrites Jbilet Winselwan (JW-2), Murchison, and Santa Cruz. Also included are spectra collected under the same analytical conditions for cronstedtite (BM52294), saponite (BM1938, 21), and San Carlos olivine taken from the NHM mineral collection. The meteorites have features at ~10 and ~22 μm from the phyllosilicates, and ~11.2 and ~16.3 μm from olivine. Jbilet Winselwan has features at ~8.6 μm, ~8.9 μm, ~14.8 μm, and ~16.8 μm from gypsum.

fragments with cracks containing secondary alteration products, it was designated a low weathering grade of W1, consistent with minor oxidation of metal and sulfides (Ruzicka et al. 2015). In the sample acquired by the NHM, white evaporites and sand are visible by eye within cracks and fractures. However, in our SEM investigations, we did not observe significant grain corrosion or infilling of cracks and fractures by rusts and Fe-oxides, suggesting only minimal terrestrial weathering.

The bulk chemical composition of Jbilet Winselwan is enriched in Ca, Sr, Ba, Li, and U (Table 4; Fig. 8b). Enrichments in the same elements were reported in samples of Jbilet Winselwan analyzed by Göpel et al. (2015) and Friend et al. (2018), and are characteristic of hot desert weathering (Barrat et al. 1999, 2001, 2003; Stelzner et al. 1999; Crozaz and Wadhwa 2001; Crozaz et al. 2003; Hezel et al. 2011). Calcium, Sr, Ba, Li, and U are very mobile in fluids and can be easily transferred from the surrounding soil into the meteorite as terrestrial sulfates and carbonates that are precipitated at the surface or fill cracks and fractures. The initial stages of hot desert weathering are expected to be rapid, with the uptake of mobile elements occurring in as few as 19 yr after the meteorite has landed on Earth (Gibson and Bogard 1978; Velbel 2014), with other examples showing similar effects in less than a century (Barrat et al. 1999). Sulfates are observed in the mid-IR spectra of Jbilet Winselwan (JW-2). A sulfate abundance of ~1 vol% is within the range that we have previously measured using PSD-XRD in CM chondrites (0.5–10 vol% in ~30% of all analyzed CMs; Howard et al. 2009, 2011, 2015; King et al. 2017), although Jbilet Winselwan is the first in which we have identified both gypsum ($CaSO_4 \cdot 2H_2O$) and anhydrite ($CaSO_4$), presumably because it was regularly subjected to temperatures >40 °C.

REE Enrichments

In our fragment of Jbilet Winselwan, we see enrichments of the REEs Ho, Er, and Lu, plus Y, Zr, Hf, Th, and Ta that were not reported in the samples analyzed by Göpel et al. (2015). Anomalies in REE abundances in Jbilet Winselwan were reported by Friend et al. (2018), who attributed them to "contamination" of their sample by ultrarefractory

Table 4. Bulk major element composition (wt%) of Jbilet Winselwan (JW-4) measured by ICP-OES. Also provided are the compositions of two of the least altered CM chondrites, EET 96029 and Paris, and two CM chondrite falls, Maribo and Murchison.

	Jbilet Winselwan[a]	EET 96029[a]	Paris[b]	Maribo[c]	Murchison[d]
SiO_2	28.3 (0.3)	26.0 (0.1)	28.72	29.35	28.84
TiO_2	0.102 (0.002)	0.088 (0.001)	0.10	0.11	0.11
Al_2O_3	2.68 (0.04)	2.27 (0.01)	2.07	2.09	2.19
Fe_2O_3	29.3 (0.2)	27.8 (0.2)	32.05	27.69	30.60
MgO	18.0 (0.2)	18.5 (0.1)	19.83	20.07	20.13
CaO	4.79 (0.04)	1.72 (0.01)	1.61	1.82	1.79
Na_2O	0.654 (0.008)	0.280 (0.003)	0.67		0.58
P_2O_5	0.241 (0.003)	0.215 (0.0003)	0.28	0.23	0.24

[a]This work; values are averages of three replicate analyses, with the standard deviation given in parentheses.
[b]Data taken from Hewins et al. (2014).
[c]Based on X-ray fluorescence from Haack et al. (2012).
[d]Values taken from Wolf and Palme (2001), Kallemeyn and Wasson (1981), and Mittlefehldt and Wetherill (1979).

inclusions (Fig. 8). The enrichment of Ho, Er, and Lu measured in our sample can be explained as a volatility-controlled signature; these elements are more refractory than other REEs under canonical solar nebular conditions and if a condensate is removed during condensation of REEs, then they will show an enrichment in these elements relative to CI abundances. This is an ultrarefractory signature, complementary to the more commonly observed Group II pattern (e.g., Davis and Grossman 1979). The enrichment of Ho, Er, and Lu suggests that the fragment of Jbilet Winselwan we analyzed contained an ultrarefractory CAI (perhaps similar to those observed in other CMs; Simon et al. 1996) that has affected the REE pattern. The likely presence of CAIs in our sample could also explain the elevated abundances of Y, Zr, Hf, Th, and Ta.

Degree of Aqueous Alteration

Microscale Properties

The CM chondrites experienced low-temperature (<100 °C) aqueous alteration when accreted ices melted on the asteroid parent body(ies) (Brearley 2006). The process was not uniform and the CM chondrites range from mildly altered type 2 meteorites to almost completely hydrated type 1 meteorites (Zolensky et al. 1997; Rubin et al. 2007; Howard et al. 2015). Defining the petrologic subtype of individual CM chondrites provides an important framework for understanding the physical and geochemical conditions of the aqueous alteration. The most widely used scheme classifies CM chondrites from 3.0 (unaltered) to 2.0 (completely altered) based on a number of petrographic and geochemical indicators including the abundance of silicates and oxides, metal in chondrules/matrix, and sulfides, and the composition of tochilinite–cronstedtite intergrowths (TCI, formerly referred to as poorly characterized phases, or PCP) and carbonates (Rubin et al. 2007). Using several of these properties, Friend et al. (2018) proposed that Jbilet Winselwan is a petrologic subtype 2.6–2.5.

On the Rubin et al. (2007) scale most CM chondrites are classified as 2.7 to 2.0 and are characterized by abundant phyllosilicates. The mineralogy of even the least altered CM chondrite, Paris (2.9–2.7), is dominated by phyllosilicates (Hewins et al. 2014; Rubin 2015). The high abundance of phyllosilicates in Jbilet Winselwan therefore indicates that its petrologic subtype is ≤2.9.

Metal (estimated at <1 vol%) was observed in the chondrules and matrix of the thin sections of Jbilet Winselwan that we studied, in agreement with the study of Pernet-Fisher et al. (2014). Friend et al. (2018) reported a metal abundance of ~1 vol% in Jbilet Winselwan. Metal is highly reactive and one of the first primary phases to alter during hydration (e.g., Hanowski and Brearley 2000); it is usually present at >1 vol% within the least altered CM chondrites (e.g., 1.2 vol% in Paris and 1.7 vol% in EET 96029, Rubin 2015; Lee et al. 2016), at <1 vol% in CM chondrites between 2.5 and 2.3, and almost absent (≤0.02 vol%) in samples of petrologic type <2.2 (Rubin et al. 2007). A metal abundance of <1 vol% in Jbilet Winselwan therefore indicates a degree of aqueous alteration from 2.5 to 2.3.

The classification of Jbilet Winselwan as a CM2.5–2.3 is supported by the abundance and mineralogy of the CAIs. CAIs are more abundant in the least altered CM chondrites, with EET 96029 (2.7) and QUE 97990 (2.6) containing 1.8 vol%, and Mighei (2.3) and Cold Bokkeveld (2.2) containing 0.3–0.6 and ~0.01 vol%, respectively (Rubin 2007; Lee et al. 2014, 2016). A CAI abundance of ≤1 vol% in Jbilet Winselwan indicates a degree of aqueous alteration consistent with CM2.5–2.3. In one of the CAIs, we find highly reactive melilite,

which was likely shielded from aqueous alteration by the more resistant diopside. In CM chondrites, melilite has only been observed in Paris (2.9–2.7) (Marrocchi et al. 2014), EET 96029 (2.7) (Lee et al. 2016), and Murchison (2.5) (McPherson et al. 1983; Simon et al. 2006), implying that rare lithologies in Jbilet Winselwan suffered a lower degree of aqueous alteration (i.e., 2.9–2.5).

The MgO/FeO ratio of CM matrix is expected to increase with the degree of aqueous alteration. For example, the MgO/FeO ratio of matrices ranges 0.35–0.42 for CM chondrite types ≥2.7, 0.39–0.46 for types 2.6–2.4, and are >0.65 for types ≤2.3 (Zolensky et al. 1993; Hewins et al. 2014; Rubin 2015; Lee et al. 2016). MgO/FeO ratios of 0.41 and 0.42 in the matrix of the Jbilet Winselwan sections JW-1-A and JW-1-E (Table 1) are therefore consistent with petrologic subtype 2.7–2.4. Similarly, S abundances in the matrix are typically higher in the least altered CM chondrites, going from ~4 wt% in Paris (2.9–2.7); 2–3 wt% in Murchison (2.5), Murray (2.5/2.4), Y-791198 (2.4), and Mighei (2.3); and ~2 wt% in Nogoya (2.2) (Zolensky et al. 1993; Rubin 2015). The average S abundance in the matrix of Jbilet Winselwan is 1.9 (±0.8) wt% suggesting a high degree of aqueous alteration, although there are likely differences between lithologies that could reflect variations in the extent of alteration (e.g., Friend et al. 2018) or loss of S during a thermal metamorphic event (s) (see the Thermal Metamorphism section).

In the probe mount (JW-1-E), we identified many chondrules that were completely altered to phyllosilicates. Glassy mesostasis and metal were among the first components in chondrules to react with the fluids, before continued alteration started to replace the coarser Mg-rich olivine and pyroxene grains (Hanowski and Brearley 2001; Velbel et al. 2012, 2015). Chondrules that are entirely hydrated are typically found in the most altered CM chondrites (CM2.0; Rubin et al. 2007). Evidence for a high degree of aqueous alteration in some regions of Jbilet Winselwan was also reported by Pernet-Fisher et al. (2014), who measured FeO/SiO_2 ratios in TCIs consistent with CM alteration from 2.3–2.0 on the Rubin et al. (2007) scale. The presence of both mildly (>2.5) and severely (<2.5) altered lithologies at the mm- to cm-scale is consistent with Jbilet Winselwan being a breccia.

Bulk Properties

Due to the challenges associated with characterizing fine-grained and heterogeneous materials in thin section it is often worth considering "bulk" properties when defining the petrologic subtypes of CM chondrites. Using PSD-XRD several studies have reported how the

Table 5. Trace element abundances (μg g^{-1}) measured in Jbilet Winselwan (JW-5) in this study (ICP-MS), by Göpel et al. (2015), and by Friend et al. (2018).

	Jbilet Winselwan[a]	Jbilet Winselwan[b]	Jbilet Winselwan[c]	Paris[d]	Murchison[e]
Li			2.96	1.6	1.7
Be		0.0300	0.03	0.0315	
P		1021	1129	1086	
K		525	561	380	
Sc	9.26	8.77	11.96	8.38	8.39
Ti		635	632	628	634
V	64.3	68.6	72.3	72.1	70
Cr	2677	3154	3170	2861	
Mn		1758	1656	1575	
Co	564	601	604	651	
Ni	12,020	11,142	13,850	14,170	
Cu	121	116	112	128	116
Zn	147	188	141	180	191
Ga	7.71	8.1	8.03	7.71	7.34
Ge	22.1				
Rb	1.29	1.37	1.52	1.72	1.66
Sr	108	91.35	42.29	10.79	10.30
Y	4.36	2.35	2.66	2.11	2.18
Zr	13.8	5.14	5.23	4.83	5.1
Nb	0.369	0.388	0.39	0.384	0.41
Mo	1.75				
Cd	0.217				
Sn	1.31				
Cs	0.087	0.140	0.17	0.131	0.127
Ba	15.6	13.61	6.16	3.24	3.23
La	0.377	0.382	0.38	0.329	0.314
Ce	0.948	0.962	0.91	0.833	0.815
Pr	0.139	0.139	0.14	0.126	0.124
Nd	0.712	0.699	0.69	0.644	0.635
Sm	0.218	0.226	0.22	0.211	0.209
Eu	0.0827	0.0843	0.08	0.0797	0.079
Gd	0.314	0.299	0.39	0.286	0.282
Tb	0.0562	0.054	0.07	0.0523	0.052
Dy	0.404	0.364	0.49	0.351	0.351
Ho	0.132	0.0813	0.11	0.0769	0.079
Er	0.543	0.235	0.28	0.225	0.231
Tm	0.0396		0.03	0.0355	0.036
Yb	0.234	0.236	0.24	0.231	0.229
Lu	0.0993	0.0347	0.04	0.0332	0.034
Hf	0.442	0.146	0.15	0.144	0.155
Ta	0.0315	0.0196	0.02	0.0192	
W		0.167	0.15	0.073	0.18
Tl	0.0566				
Pb	1.82	1.88	1.55	1.51	
Th	0.0627	0.0418	0.05	0.0386	0.039
U	0.0257	0.0271	0.02	0.0101	0.0098

[a]This work; values are the average of two replicates.
[b]Values taken from Göpel et al. (2015).
[c]Values are taken from Friend et al. (2018) and are the average of two samples.
[d]Values taken from Hewins et al. (2014).
[e]Values taken from Friedrich et al. (2002) and adjusted to the same standards as Barrat et al. (2012).

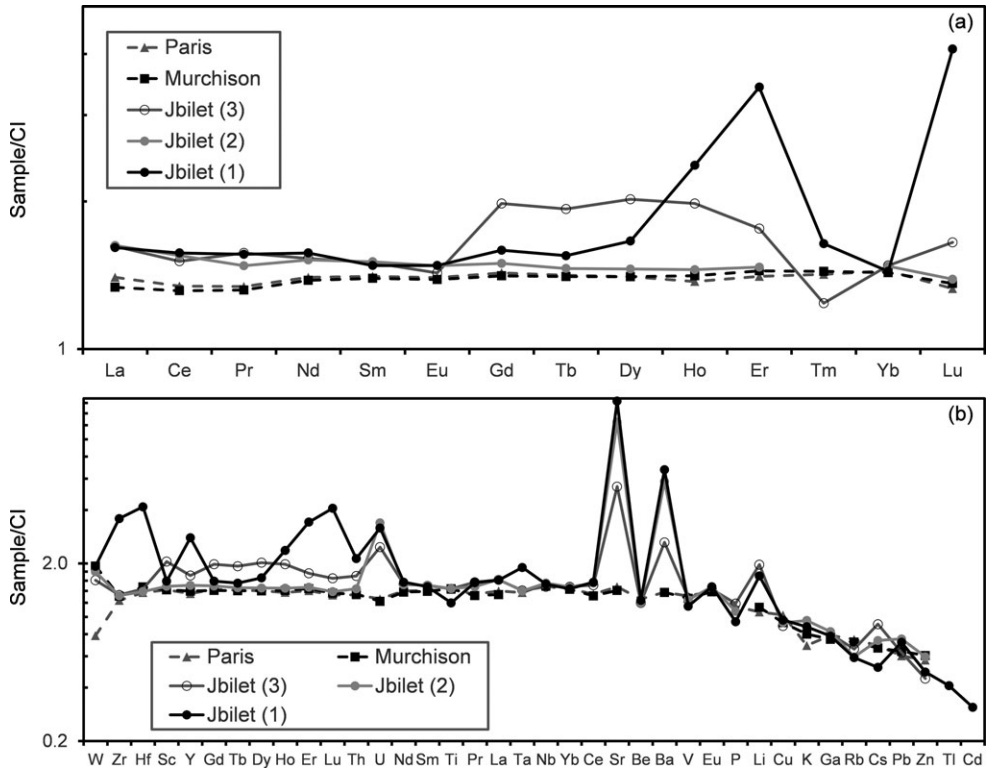

Fig. 8. REE (a) and other trace element (b) abundances in the CM chondrites Jbilet Winselwan, Paris, and Murchison. Data for Jbilet Winselwan are from (1) this study, (2) Göpel et al. (2015), and (3) Friend et al. (2018). Data for Paris are taken from Hewins et al. (2014), and for Murchison from Friedrich et al. (2002). The abundances are normalized to the CI values of Barrat et al. (2012).

Table 6. C and N abundances and isotopic composition (1σ errors given in parentheses), and He concentrations from stepped combustion of ~5 mg of Jbilet Winsewlan (JW-6).

Temperature (°C)	C (ppm)	$\delta^{13}C$	N (ppm)	$\delta^{15}N$	C/N	^{4}He (mL g^{-1})
200	267.9	−11.5 (1.4)	9.5	−6.3 (0.9)	33	
300	1332.9	−9.4 (2.4)	32.8	13.0 (1.0)	47	1.5E−06
400	2234.8	−2.1 (1.1)	29.8	23.5 (0.9)	87	1.7E−06
500	4953.3	−2.3 (0.3)	135.9	30.3 (1.0)	43	3.4E−06
600	5866.0	−8.8 (0.2)	475.9	41.5 (1.2)	14	1.5E−05
700	3858.9	−12.5 (0.2)	197.1	38.0 (1.0)	23	2.6E−05
800	1243.3	−10.2 (0.1)	25.6	35.8 (0.7)	57	1.2E−05
900	84.2	45.8 (0.2)	3.4	25.1 (1.0)	29	5.4E−07
1000	55.3	51.9 (0.2)	3.1	18.1 (1.0)	21	3.1E−07
1100	24.6	146.3 (0.1)	1.9	−20.5 (1.0)	15	2.1E−07
1200	13.1	262.9 (0.1)	1.3	6.9 (1.1)	12	
1300	6.8	56.9 (0.2)	0.6	13.2 (1.0)	13	
1400	4.4	−17.1 (0.3)	0.3	16.5 (0.8)	18	
	19945.5	−6.5	917.3	36.5	21.7	6.1E−05

bulk modal mineralogy of CM chondrites (~50–200 mg chips) changes with the degree of aqueous alteration (Howard et al. 2009, 2011, 2015; King et al. 2017). Howard et al. (2009) demonstrated that even for the CM breccias, analyses of separate "bulk" samples of the same meteorite display only minor (<5 vol%) variations in modal mineralogy. The abundance of phyllosilicate relative to anhydrous silicate increases with hydration (Fig. 11), leading Howard et al. (2015) to propose the phyllosilicate fraction (PSF = total phyllosilicate

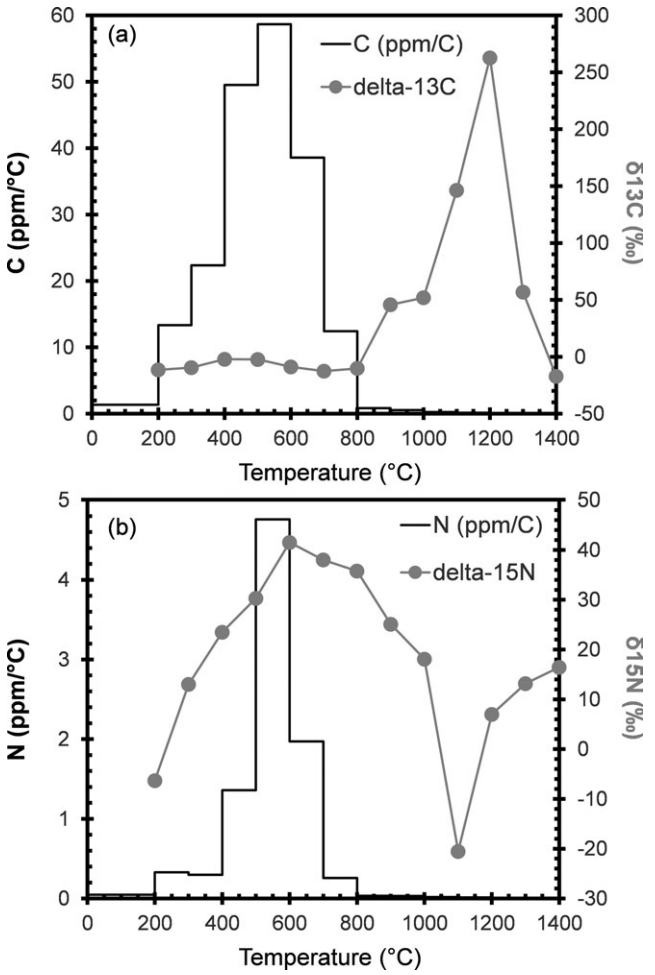

Fig. 9. Stepped combustion profiles for (a) carbon and (b) nitrogen in the Jbilet Winselwan (JW-6) CM chondrite.

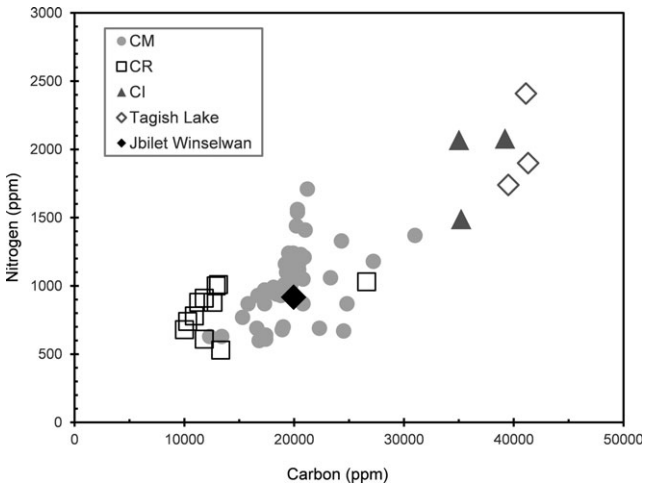

Fig. 10. Carbon and nitrogen abundances in Jbilet Winselwan (JW-6) compared to CM, CR, CI chondrites and the ungrouped meteorite Tagish Lake. Data for the CM, CR, CI, and Tagish Lake meteorites are taken from Alexander et al. (2012).

abundance/[total anhydrous silicate + total phyllosilicate abundance]) as a method for classifying CM chondrites. The PSF is converted into petrologic type from 3.0 (unaltered) to 1.0 (complete hydration), with higher resolution subtypes within this defined by 5 vol% increments in phyllosilicate abundance (i.e., a type 3.0 chondrite has a PSF of <0.05, a type 2.0 of 0.5, and type 1.0 of >0.95).

If we assume that the noncrystalline component in Jbilet Winselwan was phyllosilicates prior to a thermal metamorphic event(s), we calculate a PSF of 0.78. On the Howard et al. (2015) scale, this corresponds to a petrologic subtype of 1.5 (which from eq. 2 in Howard et al. [2015] translates as type 2.4 on the Rubin et al. [2007] scale), similar to CM chondrites such as Murchison and Murray.

Trends in the abundance of some minor phases in CM chondrites are also useful for inferring the extent of aqueous alteration (King et al. 2017). For example, Fig. 12 shows that magnetite abundances are correlated with the degree of alteration and that Jbilet Winselwan is consistent with other CM chondrites of petrologic subtype 1.5 (on the Howard et al. [2015] scale). We did not detect metal in the PSD-XRD pattern of either JW-2 or JW-3, suggesting that it is present at <1 vol% in bulk (~50 mg) samples. Metal has previously been identified in the weakly altered meteorites EET 96029 (0.3 vol%), QUE 97990 (0.2 vol%), and Y-791198 (0.2 vol%) (all 1.6 on Howard et al. [2015] scale), but is otherwise rarely observed in CM chondrites by bulk methods (Howard et al. 2009, 2011, 2015; King et al. 2017). The absence of metal in the PSD-XRD patterns of JW-2 and JW-3 is consistent with alteration at <1.6 on the Howard et al. (2015) scale (as is inferred from the PSF), although we note that metal was identified in LAP 03718 (0.2 vol%) and LAP 02336 (0.4 vol%), which experienced a comparable degree of alteration to Jbilet Winselwan (type 1.5 and 1.4, respectively) (Howard et al. 2015).

An additional classification scheme based on the bulk (2–10 mg) H contents (in H_2O and OH) of CM chondrites was proposed by Alexander et al. (2013). Again, the scale goes from type 3.0 (unaltered) to 1.0 (completely altered), with the more altered CM chondrites containing higher abundances of H. This is attributed to the abundance of phyllosilicates, and the two properties are reasonably well correlated (Alexander et al. 2013). If we assume that all of the mass loss between 200 and 770 °C in our TGA measurements was due to dehydration and dehydroxylation of Fe-(oxy) hydroxides and phyllosilicates, we estimate an H abundance of 1.0 wt% for JW-2 and 1.2 wt% for JW-3. These H abundances are consistent with CM chondrites

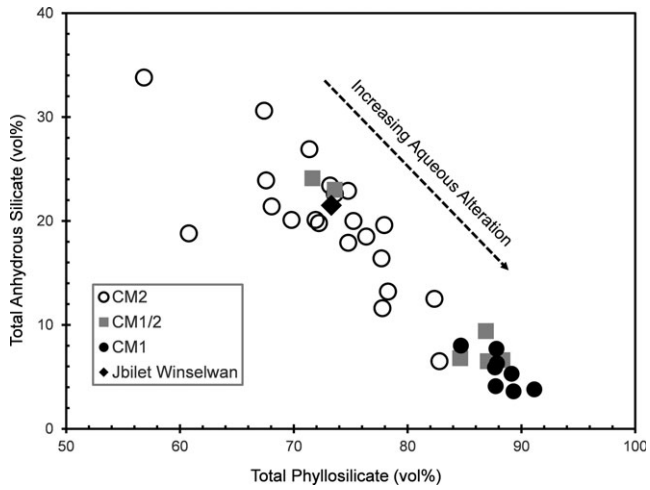

Fig. 11. Total phyllosilicate and anhydrous silicate abundance in Jbilet Winselwan (average of JW-2 and JW-3) compared to PSD-XRD data for 35 CM chondrites. CM data are taken from Howard et al. (2009, 2011, 2015) and King et al. (2017).

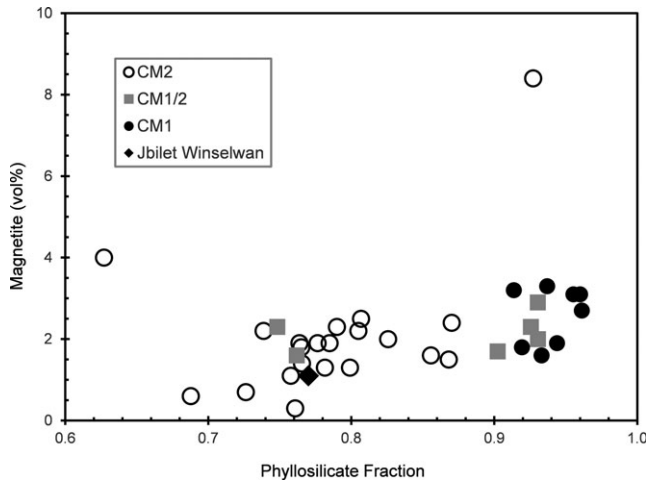

Fig. 12. Variations in the abundance of magnetite with increasing aqueous alteration in CM chondrites. Abundances for Jbilet Winselwan are the average of two samples (JW-2 and JW-3); other CM data are taken from Howard et al. (2009, 2011, 2015) and King et al. (2017).

containing ~70 vol% phyllosilicate (i.e., similar PSF on Fig. 13), and correspond to petrologic subtypes 1.6 and 1.3 on the Alexander et al. (2013) scale. However, TGA-derived H abundances are often 10–15% higher than those measured using mass spectrometry (as in the Alexander et al. [2013] study) due to additional mass loss in this temperature region from the breakdown of Fe-sulfides and refractory organics (Garenne et al. 2014; King et al. 2015b). To our knowledge, the H contents of Jbilet Winselwan have not been determined using mass spectrometry. Applying a correction of 15% to our TGA

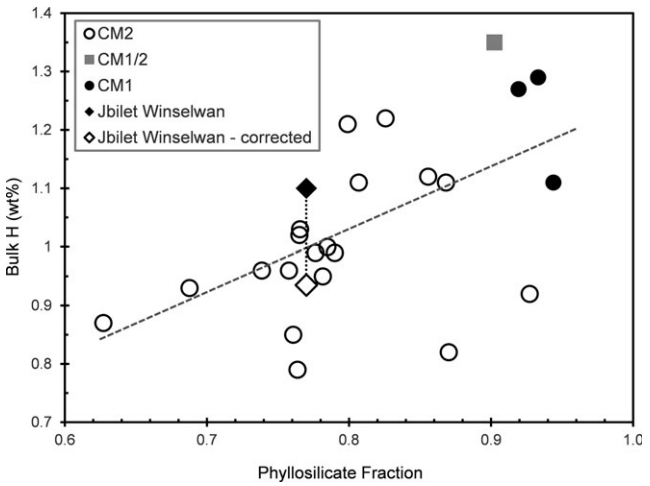

Fig. 13. Phyllosilicate fraction versus bulk H contents for CM chondrites. The H abundance of Jbilet Winselwan (average of JW-2 and JW-3 samples) was determined using TGA and has been corrected (open diamond, with correction shown as a dashed black line) by 15% due to the breakdown of Fe-sulfides, carbonates, and refractory organics in the 200–770 °C temperature region (see text for details). For the other CM chondrites, the H abundances are taken from Alexander et al. (2013) and were determined using mass spectrometry; phyllosilicate fractions are from Howard et al. (2009, 2011, 2015) and King et al. (2017). The data show a positive linear correlation (dashed gray line).

data results in a H abundance of 0.85 for JW-2 (type 1.8) and 1.02 for JW-3 (type 1.5), taking them slightly below the trend line on Fig. 13, but still in agreement with CM chondrites of the same petrologic subtype.

Finally, Beck et al. (2014a) tracked the extent of aqueous alteration in CM chondrites using mid-IR spectra. They devised a mineralogical indicator based on the relative intensities of the phyllosilicate and olivine features at ~10 μm and ~11.2 μm, respectively. Aqueous alteration converts olivine to phyllosilicates, resulting in a lower 11.2 μm/10 μm ratio. Qualitatively applying the same criteria to our mid-IR spectra (Fig. 7), we infer an alteration sequence of Jbilet Winselwan (JW-2) < Murchison < Santa Cruz.

Thermal Metamorphism

Zolensky et al. (2016) identified distinct lithologies in Jbilet Winselwan that experienced thermal metamorphism. Several lines of evidence for post-aqueous alteration heating of these lithologies were described, including the "spongy" texture of matrix and aggregates, the presence of fine-grained olivine recrystallized from phyllosilicates, and partially melted Fe-sulfides. High EMPA totals consistent with dehydration of phyllosilicates were also noted but are not apparent in our analyses of the matrix in the Jbilet Winselwan samples JW-1-A and JW-1-E (Table 1).

The effects of thermal metamorphism in Jbilet Winselwan are evident at the bulk scale. We see no coherent phyllosilicate diffraction for JW-2 and JW-3 (Fig. 5), consistent with other thermally altered CM chondrites analyzed in our laboratory (e.g., King et al. 2015a, 2015c). In addition, the Fe-sulfide (pyrrhotite/troilite) peak at ~43° (2θ, Cu $K\alpha_1$) is much broader than for non-heated CM chondrites, suggesting possible melting and initial recrystallization to very fine grain sizes (Nakamura 2005).

Nakamura (2005) proposed four heating stages (I–IV) for the aqueously altered and thermally metamorphosed carbonaceous chondrites based upon their XRD patterns. Using this scheme, Nakamura et al. (2014) classified Jbilet Winselwan as a stage II meteorite, representing heating between 250 and 500 °C. Our observations agree with this finding; both JW-2 and JW-3 contain an abundant highly disordered and/or very fine-grained phase that was likely phyllosilicates, but we do not see any evidence for recrystallized olivine. At temperatures >500 °C phyllosilicates can undergo dehydration to form fine-grained and/or poorly crystalline olivine, which results in broad diffraction peaks. However, the sharp olivine peaks we observe in JW-2 and JW-3 are typical of unheated CM chondrites and indicate that lithologies in Jbilet Winselwan were heated to a temperature no higher than ~500 °C.

Tochilinite was not identified in the XRD patterns of JW-2 and JW-3, although it was sometimes seen both within our thin sections (Fig. 2c) and those studied by Friend et al. (2018). Howard et al. (2009, 2011) observed a tochilinite peak in the XRD patterns of all CM2 chondrites, but it is usually absent from the CM1s (King et al. 2017). Because lithologies in Jbilet Winselwan are not fully hydrated (see the Degree of Aqueous Alteration section), we suggest that the low abundance of tochilinite is due to thermal metamorphism. This implies that some lithologies in Jbilet Winselwan were heated to at least ~120 °C, the temperature at which tochilinite breaks down (Zolensky et al. 1997).

A metamorphic temperature range of ~120–500 °C is supported by a notable loss of volatiles in Jbilet Winselwan. For example, while the C and N abundances and stepped combustion profiles for Jbilet Winselwan are typical of unheated CM chondrites, there is a depletion in the amount of ^{4}He released at <600 °C (Fig. 14). The DTG curves of JW-2 and JW-3 display low mass loss (5.5–6.4 wt%) from ~200 to 650 °C (Fig. 6) when compared to unheated CM2 chondrites of similar petrologic subtype (e.g., Murchison), which typically lose ~9 wt% in the same temperature region largely due to the dehydration of

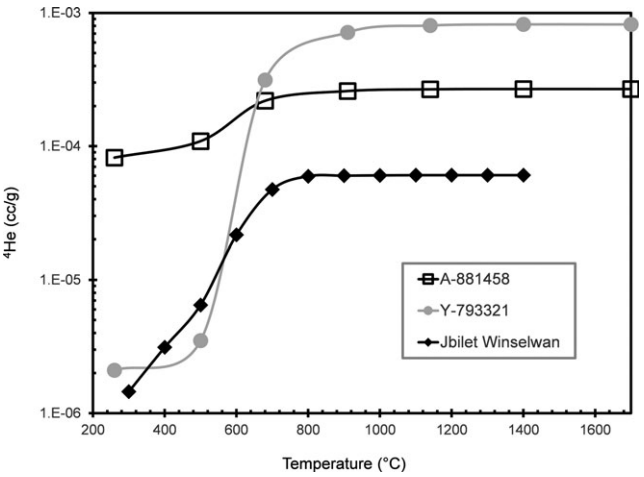

Fig. 14. Cumulative ^{4}He gas release during stepped combustion for samples of Jbilet Winselwan (JW-6, this study), plus the heated CM chondrites A-881458 (stage I) and Y-793321 (stage II) (data from Nakamura 2006).

Fe-rich phyllosilicates (Garenne et al. 2014). We also find that the volatile trace elements Cs, Tl, and Cd are depleted in Jbilet Winselwan (Fig. 8b). The artificial heating experiments of Wang and Lipschutz (1998) using Murchison showed that these elements are lost during thermal metamorphism at temperatures >400 °C. Cadmium, as the most volatile, is a particularly sensitive indicator of thermal metamorphism in CM chondrites, and its level of depletion (~×3.0 relative to CI abundances) in Jbilet Winselwan is consistent with classification as a stage II meteorite (Nakamura 2005).

Based on our XRD observations and the loss of multiple volatile species, we propose that some lithologies in Jbilet Winselwan likely experienced a metamorphic event at 400–500 °C prior to arrival on Earth. The heating was clearly heterogeneous and did not affect all regions within Jbilet Winselwan equally. For example, the Meteoritical Bulletin entry for Jbilet Winselwan describes coherent X-ray diffraction from phyllosilicates, suggesting that they are not all dehydrated, and in contrast to this study, Göpel et al. (2015) and Friend et al. (2018) did not observe depletions in the volatile trace elements such as Cs (they did not report Tl and Cd abundances).

Carbonates

Carbonates are present within CM chondrites at 1–5 vol%; in the CM2s, calcite is the main carbonate phase (Howard et al. 2009, 2011, 2015), whereas dolomite is more abundant than calcite in the CM1s (King et al. 2017). We did not detect either calcite or dolomite in the XRD patterns of JW-2 and JW-3,

suggesting that the carbonate abundance in these samples is <1 vol%. We also identified few carbonate grains in the thin sections and probe mount of Jbilet Winselwan, in agreement with the findings of Pernet-Fisher et al. (2014).

A low carbonate abundance in Jbilet Winselwan is inferred from the carbon stepped combustion profile (measured in vacuum); there was no local maximum in $\delta^{13}C$ at 500–600 °C (Fig. 9a), which in other CM chondrites indicates the presence of $\delta^{13}C$-enriched extraterrestrial carbonates (e.g., Grady et al. 2002). Terrestrial weathering could be an issue and C (and N) abundances are often depleted in carbonaceous chondrites recovered from the Sahara (Ash and Pillinger 1995). However, the C and N abundances in Jbilet Winselwan fall within the range of other CM chondrites (Fig. 10). Similarly, the TGA mass loss of JW-2 (1.6 wt%) and JW-3 (1.3 wt%) between 770 and 900 °C (Table 3) related to the breakdown of carbonates was typical of other CM chondrites (Garenne et al. 2014). If we assume that all of the mass loss between 770 and 900 °C was CO_2 released from calcite, this gives an abundance of 3–4 vol% for JW-2 and JW-3.

Jbilet Winselwan appears to have a heterogeneous distribution of carbonates, which is not an uncommon characteristic of CM chondrite breccias (Alexander et al. 2015; King et al. 2017). We rule out variations in the degree of thermal metamorphism as the cause because Jbilet Winselwan was probably heated to 400–500 °C (see the Thermal Metamorphism section), which is below the expected breakdown temperature of carbonates (Nozaki et al. 2006; Rodriguez-Navarro et al. 2009). The heterogeneous distribution of carbonates may instead result from a parent body process such as variable accretion and melting of C-rich ices (e.g., HCN, CO_2, CO), differences in the local mineralogy (e.g., number of CAIs, abundance of organic species), or the effects of impact brecciation. Weathering could also have played a role, with a terrestrial carbonate component hinted at by elevated Ca abundances and low $\delta^{13}C$ compositions in bulk samples (Grady et al. 2002).

Alteration History of Jbilet Winselwan

Jbilet Winselwan formed when accreted ices melted on its parent body and reacted with an anhydrous silicate component. The Mn-Cr ages of carbonates in CM chondrites indicate that the aqueous alteration started ~4.56 Gyr ago, with the final precipitation events occurring ~10 Myr after that (Endress et al. 1996; De Leuw et al. 2009; Fujiya et al. 2012). Based on mineralogy, and isotopic and chemical compositions it is often assumed that the CM chondrites are derived from a single, complex asteroid (e.g., Lindgren et al. 2017). However, CM-like material is found throughout the solar system (McCord et al. 2012; DeMeo and Carry 2015) and recent studies suggest that the CM chondrites could originate from multiple parent bodies (e.g., Takenouchi et al. 2014).

Our data show that like many other CM chondrites, Jbilet Winselwan contains lithologies that experienced varying degrees of aqueous alteration. These variations have been attributed to differences in the temperature and/or water/rock ratio under which the alteration occurred (McSween 1979; Clayton and Mayeda 1984, 1999; Tomeoka and Buseck 1985; Zolensky et al. 1989, 1997; Browning et al. 1996; Hanowski and Brearley 2001; Rubin et al. 2007; King et al. 2017). Temperatures are modeled to be higher within the interior of a parent body, or at near-surface regions heated by convection (e.g., Palguta et al. 2010) and impact events (e.g., Lee and Nicholson 2009). Variable water/rock ratios may have resulted from heterogeneous accretion of ices, transport of fluids along cracks and fractures (Rubin 2012), or differential compaction (Alexander et al. 2013).

Some lithologies in Jbilet Winselwan show evidence for thermal metamorphism at temperatures of 400–500 °C. The presence of a dehydrated phyllosilicate phase indicates that the heating occurred either simultaneously with, or more likely after, aqueous alteration. However, our observations also demonstrate that the heating was heterogeneous and that some regions in Jbilet Winselwan were either heated to lower temperatures (<400 °C), for a shorter period of time, or avoided metamorphism altogether.

The lithologies in Jbilet Winselwan experienced complex aqueous and thermal processing before being mixed into a final breccia and ejected from the parent body. Most CM chondrites are regolith breccias formed by impacts, although in Jbilet Winselwan we do not observe any other signs of impact such as olivine fracturing or deformed chondrules. Regolith breccias should retain implanted solar wind noble gases having spent a period of time at the surface of their parent body(ies) but Meier et al. (2016) reported that Jbilet Winselwan does not contain any solar wind noble gases. The solar wind component is known to be heterogeneously distributed in CM chondrites, although the gases are predominantly located within the clastic matrix (Nakamura et al. 1999). Thermal metamorphism at ~500 °C is not expected to fully remove any implanted solar wind component (Nakamura 2006), so it is possible that Meier et al. (2016) analyzed an unbrecciated, matrix-poor region of Jbilet Winselwan. Alternatively, Jbilet Winselwan may sample the interior of the parent body and did not reside at the surface for

any significant amount of time. This is similar to several other aqueously and thermally altered carbonaceous chondrites (e.g., Y-82162) that have been interpreted as impact breccias but do not contain solar wind noble gases (Nagao et al. 1984; Weber and Schultz 1991; Nakamura et al. 2000).

There are now >20 CM chondrites identified as having experienced post-hydration thermal metamorphism, but the mechanism, timing, and duration of the heating remains poorly constrained (Nakamura 2005; Tonui et al. 2014). Mineral textures and organic structures in the heated CM chondrites indicate that the metamorphism was short-lived, perhaps on the order of hours to several years (Nakato et al. 2008; Yabuta et al. 2010). This seemingly rules out the radioactive decay of ^{26}Al as the cause because it is expected to heat asteroids on a time scale of $>10^6$ yr (Miyamoto 1991). Alternative options include shock heating from impacts (Lunning et al. 2016) or solar radiation (Chaumard et al. 2012). We prefer shock heating as depending on the size, velocity, and composition of the impactor and target material, it could produce regions on the parent body with very different thermal histories (Bland et al. 2014). There is evidence for heterogeneous heating in Jbilet Winselwan, and also the Sutter's Mill meteorite (Beck et al. 2014b), but otherwise the effects are rarely seen in CM chondrites (Lunning et al. 2016), possibly because water-rich asteroids are expected to disrupt in large collisions and not preserve an impact record (Scott et al. 1992). Nevertheless, in Jbilet Winselwan, there are aggregates of well-sorted olivine grains, vesicular amorphous beads, and melted Fe-sulfide masses with matrix olivine grains injected into them, that may have formed through repeated impacts and rapid heating (Zolensky et al. 2016).

Many of the key properties of Jbilet Winselwan are similar to the heated CM chondrite Y-793321; they contain a dehydrated phyllosilicate phase and primary olivine and enstatite, plus H_2O (9.2 wt% in Y-793321), C (1.78 wt%), and thermally mobile trace element abundances, and O isotopic compositions, that all fall within the range of other CM chondrites (Nakamura 2006). Both meteorites underwent a low degree of aqueous alteration before impact brecciation and heating to <500 °C. Y-793321 contains solar wind noble gases, leading Nakamura (2006) to classify it as a sample of dehydrated regolith from the surface of a water-rich asteroid. Nakamura (2006) concluded that the extent of heating, and the subsequent loss of volatiles (e.g., H_2O and ^{4}He) in Y-793321 were the equivalent of a single 15 GPa impact, and we infer a comparable history for Jbilet Winselwan. In contrast, the CM chondrite EET 96029 was also subjected to a very low degree of aqueous alteration followed by brecciation and thermal metamorphism at temperatures of 400–600 °C, but contains no evidence for shock, hinting that it was instead heated by solar radiation (Lee et al. 2016).

Relationship with Asteroid Surfaces

Jbilet Winselwan is a CM chondrite that experienced varying degrees of both aqueous and thermal alteration on an asteroid parent body. Thermal metamorphism may have occurred simultaneously with, or after hydration, and was caused by impacts and/or solar radiation, processes active at the surfaces of asteroids. The visible and near-IR reflectance spectra of heated CM chondrites share a number of features with some low albedo, primitive C-type asteroids (Hiroi et al. 1993, 1996). This suggests that the surfaces of these asteroids are likely to host a mixture of hydrated and dehydrated phases, and that heated CM chondrites such as Jbilet Winselwan are good analogs for the types of materials that will be encountered by the Hayabusa-2 and OSIRIS-REx sample-return missions to the near-Earth asteroids Ryugu and Bennu, respectively.

Recently, Meier et al. (2016) raised the possibility that Jbilet Winselwan could be a fragment from the Veritas family of asteroids. Residing in the outer Main Belt (~3.2 AU), the Veritas family formed through the catastrophic disruption of a porous, ~140 km diameter parent body ~8.3 (±0.5) Myr ago, and may be the source of up to 25% of the interplanetary dust that reaches Earth (Nesvorný et al. 2003). Asteroids in the Veritas family all fall within the C complex taxonomic group (specifically C-, Ch-, and Cg-types) that has been linked to the CM chondrites (e.g., Cloutis et al. 2011). Meier et al. (2016) found that the cosmic-ray exposure (CRE) age of Jbilet Winselwan (6.6 ± 1.7 Myr) is much longer than is typical for CM chondrites (usually <2 Myr), and within the uncertainty, is in good agreement with the timing of the Veritas breakup event. There are a few CM chondrites with comparable CRE ages, including Santa Cruz, which based on its XRD pattern (Fig. 5) was not thermally altered, and Y-793321, a heated (stage II) CM chondrite regolith breccia (Nakamura 2006).

Landsman et al. (2016) collected 5–14 μm emissivity spectra for Veritas family asteroids, identifying a broad feature at ~10 μm that they attributed to the presence of a fine-grained and/or porous silicate regolith. Figure 15 compares mid-IR spectra for Jbilet Winselwan, Santa Cruz, and Y-793321 to the 10 μm feature for six Veritas family asteroids. The position of the feature for Jbilet Winselwan, Santa Cruz, and Y-793321 (~10 μm) best matches family members 2934 Aristophanes (9.9 ± 0.3 μm) and 5592 Oshima

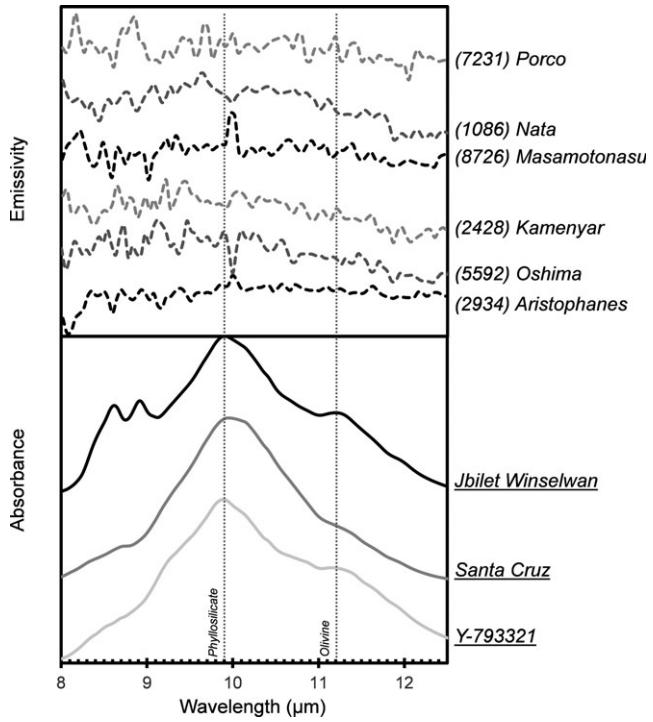

Fig. 15. Comparison of transmission mid-IR spectra for the CM chondrites Jbilet Winselwan, Santa Cruz (both this study), and Y-793321 (analyzed under the same conditions by King et al. 2015c), and the ~10 μm emissivity feature for six Veritas asteroids (data taken from Landsman et al. 2016). The spectral contrast of the 10 μm feature for the asteroids is <4%, and band centers were calculated as Aristophanes (9.9 ± 0.3 μm), Oshima (10.0 ± 0.7 μm), Kamenyar (10.2 ± 0.1 μm), Masamotonasu (10.4 ± 0.1 μm), Nata (10.4 ± 0.1), and Porco (10.5 ± 0.2 μm) (for details see Landsman et al. 2016).

(10.0 ± 0.7 μm), both of which are classified as Ch-type asteroids (Bus and Binzel 2002; Lazzaro et al. 2004). Due to the low spectral resolution and contrast, an olivine feature at ~11.2 μm cannot be reliably identified in the asteroid spectra. However, the position of the emissivity minimum has been shown to occur at longer wavelengths for less altered CM chondrites and can tentatively be used to remotely infer the degree of aqueous alteration on asteroid surfaces (McAdam et al. 2015). Landsman et al. (2016) calculated that the emissivity minimum is at 12.36 (±0.04) μm for 2934 Aristophanes and 12.47 (±0.04) μm for 5592 Oshima, consistent with a relatively low abundance of phyllosilicate (~65–70 vol%; McAdam et al. 2015). These values are in good agreement with our data for Jbilet Winselwan (~73 vol%) and also the unheated Santa Cruz (~70 vol%), highlighting the need to develop a rigorous method for remotely discriminating between dehydrated and hydrated C-type asteroid surfaces.

CONCLUSIONS

The CM carbonaceous chondrites can be used to constrain the formation and evolution of water-rich asteroids in the outer solar system. Jbilet Winselwan is one of the largest CM chondrites available for analysis and has therefore become an important sample for the meteorite community. Here, we have characterized the micro- and bulk-scale properties of Jbilet Winselwan in order to establish its alteration history and relationship with primitive asteroid parent bodies.

1. Jbilet Winselwan contains chondrules (Type I and II), CAIs and isolated fragments often surrounded by dusty rims and set within a fine-grained matrix of phyllosilicates, oxides, and sulfides. In general, its light, major, and trace element compositions fall within the ranges reported for other CM chondrites.
2. In thin sections and a probe mount of Jbilet Winselwan, we do not observe any significant grain corrosion or infilling of cracks by rust and Fe-oxides. However, white evaporites and sand are visible in hand specimen and both gypsum and anhydrite are detected in bulk XRD analysis. In addition, Jbilet Winselwan is enriched in mobile elements such as Ca, Sr, Ba, Li, and U, which is a typical feature of hot desert weathering. Our observations concur with previous studies that have designated Jbilet Winselwan with a low weathering grade of W1.
3. Petrographic observations and mineral compositions indicate that Jbilet Winselwan contains lithologies that experienced varying degrees of aqueous alteration. Based on the relatively mild alteration of chondrules, abundance of CAIs—one of which contains melilite—and metal, and the matrix composition, we infer that most lithologies were altered to petrologic type 2.7–2.4. In other lithologies, we find chondrules and CAIs completely altered to phyllosilicates, consistent with alteration to petrologic type ≤2.3. Variable aqueous alteration on the CM parent body has been attributed to differences in the temperature and/or water/rock ratio under which hydration occurred. The mixture of such diverse lithologies at the mm- to cm-scale is consistent with Jbilet Winselwan being a breccia.
4. At the bulk scale, Jbilet Winselwan contains 73 vol% of a highly disordered and/or very fine-grained phase, which we infer was phyllosilicates prior to a thermal metamorphic event(s), and 22 vol% anhydrous silicates, resulting in a phyllosilicate fraction (PSF) of 0.78. On the Howard et al. (2015) scale, this corresponds to a petrologic subtype of 1.5, which is the equivalent of type 2.4 on the Rubin et al. (2007) scale and similar to CM chondrites such as

Murchison and Murray. Estimated H abundances and mid-IR spectra of Jbilet Winselwan are also consistent with intermediately altered CM chondrites.

5. Following aqueous alteration some lithologies in Jbilet Winselwan experienced at least one thermal metamorphic event. Evidence for heating includes dehydration of the phyllosilicates, a low abundance of tochilinite, and significant depletions in He and other volatile elements. Based on the depletion of Cd and a lack of evidence for dehydration of phyllosilicates into olivine, we suggest that the peak metamorphic temperature was 400–500 °C, and was probably caused by impact heating.
6. Jbilet Winselwan samples hydrated and dehydrated materials from a primitive water-rich primitive asteroid. Meteorites such as Jbilet Winselwan may be good analogs for the types of materials that will be encountered by the Hayabusa-2 and OSIRIS-REx sample-return missions to the C complex asteroids Ryugu and Bennu, respectively. The CRE age (6.6 ± 1.7 Myr) of Jbilet Winselwan is much longer than most CM chondrites and is comparable to the breakup age of the Veritas asteroid family (Meier et al. 2016). In a simple comparison of mid-IR spectral features, we suggest that if Jbilet Winselwan is derived from the Veritas family of asteroids, the best candidates are the Ch-type asteroids 2934 Aristophanes and 5592 Oshima.

Acknowledgments—We thank Caroline Smith, Deborah Cassey, and Natasha Almeida at the Natural History Museum, UK, for help with preparing the samples used in this study. Jens Najorka and Rachel Norman are thanked for assistance with the XRD and TGA analyses, and Zoe Landsman for sharing the Veritas asteroid spectra. The IR spectra were acquired with the help of Gianfelice Cinque and Mark Frogley during experiment SM9614 at Diamond Light Source, UK. Finally, we also thank Adrian Brearley, Paula Lindgren, Kazushige Nakamura, and Michael Velbel for reviews that significantly improved the science and clarity of the manuscript. This work was funded by the Science and Technology Facilities Council (STFC), UK, through grants ST/J001473/1 and ST/M00094X/1.

Editorial Handling—Prof. Adrian Brearley

REFERENCES

Alexander C. M. O'D., Bowden R., Fogel M. L., Howard K. T., Herd C. D. K., and Nittler L. R. 2012. The provenances of asteroids, and their contributions to the volatile inventories of the terrestrial planets. *Science* 337:721–723.

Alexander C. M. O'D., Howard K. T., Bowden R., and Fogel M. L. 2013. The classification of CM and CR chondrites using bulk H, C and N abundances and isotopic compositions. *Geochimica et Cosmochimica Acta* 123:244–260.

Alexander C. M. O'D., Bowden R., Fogel M. L., and Howard K. T. 2015. Carbonate abundances and isotopic compositions in chondrites. *Meteoritics & Planetary Science* 50:810–833.

Ash R. D. and Pillinger C. T. 1995. Carbon, nitrogen and hydrogen in Saharan chondrites: The importance of weathering. *Meteoritics* 30:85–92.

Barrat J.-A., Gillet P., Lesourd M., Blichert-Toft J., and Poupeau G. R. 1999. The Tatahouine diogenite: Mineralogical and chemical effects of sixty-three years of terrestrial residence. *Meteoritics & Planetary Science* 34:91–97.

Barrat J.-A., Blichert-Toft J., Nesbitt R. W., and Keller F. 2001. Bulk chemistry of Saharan shergottite Dar al Gani 476. *Meteoritics & Planetary Science* 36:23–29.

Barrat J.-A., Jambon A., Bohn M., Blichert-Toft J., Sautter V., Göpel C., Gillet P., Boudouma O., and Keller F. 2003. Petrology and geochemistry of the unbrecciated achondrite Northwest Africa 1240 (NWA 1240): An HED parent body impact melt. *Geochimica et Cosmochimica Acta* 67:3959–3970.

Barrat J.-A., Zanda B., Moynier F., Bollinger C., Liorzou C., and Bayon G. 2012. Geochemistry of CI chondrites: Major and trace elements, and Cu and Zn isotopes. *Geochimica et Cosmochimica Acta* 83:79–92.

Beck P., Quirico E., Montes-Hernandez G., Bonal L., Bollard J., Orthous-Daunay F.-R., Howard K. T., Schmitt B., Brissaud O., Deschamps F., Wunder B., and Guillot S. 2010. Hydrous mineralogy of CM and CI chondrites from infrared spectroscopy and their relationship with low albedo asteroids. *Geochimica et Cosmochimica Acta* 74:4881–4892.

Beck P., Garenne A., Quirico E., Bonal L., Montes-Hernandez G., Moynier F., and Schmitt B. 2014a. Transmission infrared spectra (2–25 μm) of carbonaceous chondrites (CI, CM, CV-CK, CR, C2 ungrouped): Mineralogy, water, and asteroidal processes. *Icarus* 229:263–277.

Beck P., Quirico E., Garenne A., Yin Q.-Z., Bonal L., Schmitt B., Montes-Hernandez G., Chiriac R., and Toche F. 2014b. The secondary history of Sutter's Mill CM carbonaceous chondrite based on water abundance and structure of its organic matter from two clasts. *Meteoritics & Planetary Science* 49:2064–2073.

Bland P. A., Cressey G., and Menzies O. N. 2004. Modal mineralogy of carbonaceous chondrites by X-ray diffraction and Mössbauer spectroscopy. *Meteoritics & Planetary Science* 39:3–16.

Bland P. A., Zolensky M. E., Benedix G. K., and Sephton M. A. 2006. Weathering of chondritic meteorites. In *Meteorites and the early solar system II*, edited by Lauretta D. S. and McSween H. Y. Tuscon, Arizona: The University of Arizona Press. pp. 853–867.

Bland P. A., Collins G. S., Davison T. M., Abreu N. M., Ciesla F. J., Muxworthy A. R., and Moore J. 2014. Pressure-temperature evolution of primordial solar system solids during impact-induced compaction. *Nature Communications* 5:5451.

Brearley A. J. 2006. The action of water. In *Meteorites and the early solar system II*, edited by Lauretta D. S. and

McSween H. Y. Tuscon, Arizona: The University of Arizona Press. pp. 587–624.
Browning L. B., McSween H. Y., and Zolensky M. E. 1996. Correlated alteration effects in CM carbonaceous chondrites. *Geochimica et Cosmochimica Acta* 60:2621–2633.
Bus S. J. and Binzel R. P. 2002. Phase II of the small main-belt asteroid spectroscopic survey. A feature-based taxonomy. *Icarus* 158:146–177.
Chan Q. H. S., Zolensky M. E., Bodnar R. J., Farley C., and Cheung J. C. H. 2017. Investigation of organo-carbonate associations in carbonaceous chondrites by Raman spectroscopy. *Geochimica et Cosmochimica Acta* 201:392–409.
Chaumard N., Devouard B., Delbo M., Provost A., and Zanda B. 2012. Radiative heating of carbonaceous near-Earth objects as a cause of thermal metamorphism of CK chondrites. *Icarus* 220:65–73.
Clayton R. N. and Mayeda T. K. 1984. The oxygen isotope record in Murchison and other carbonaceous chondrites. *Earth and Planetary Science Letters* 67:151–161.
Clayton R. N. and Mayeda T. K. 1999. Oxygen isotope studies of carbonaceous chondrites. *Geochimica et Cosmochimica Acta* 63:2089–2104.
Cloutis E. A., Hudon P., Hiroi T., Gaffey M. J., and Mann P. 2011. Spectral reflectance properties of carbonaceous chondrites: 2 CM chondrites. *Icarus* 216:309–346.
Cressey G. and Schofield P. F. 1996. Rapid whole-pattern profile stripping method for the quantification of multiphase samples. *Powder Diffraction* 11:35–39.
Crozaz G. and Wadhwa M. 2001. The terrestrial alteration of Saharan Shergottites Dar al Gani 476 and 489: A case study of weathering in a hot desert environment. *Geochimica et Cosmochimica Acta* 65:971–978.
Crozaz G., Floss C., and Wadhwa M. 2003. Chemical alteration and REE mobilization in meteorites from hot and cold deserts. *Geochimica et Cosmochimica Acta* 67:4727–4741.
Davis A. M. and Grossman L. 1979. Condensation and fractionation of rare earths in the solar nebula. *Geochimica et Cosmochimica Acta* 43:1611–1632.
De Leuw S., Rubin A. E., Schmidt A. K., and Wasson J. T. 2009. 53Mn-53Cr systematics of carbonates in CM chondrites: Implications for the timing and duration of aqueous alteration. *Geochimica et Cosmochimica Acta* 73:7433–7442.
DeMeo F. E. and Carry B. 2015. Solar system evolution from compositional mapping of the asteroid belt. *Nature* 505:629–634.
Endress M., Zinner E., and Bischoff A. 1996. Early aqueous activity on primitive meteorite parent bodies. *Nature* 379:701–703.
Ferrat M., Weiss D. J., and Strekopytov S. 2012. A single procedure for the accurate and precise quantification of the rare earth elements, Sc, Y, Th and Pb in dust and peat for provenance tracing in climate and environmental studies. *Talanta* 93:415–423.
Friedrich J. M., Wang M.-S., and Lipschutz M. E. 2002. Comparison of the trace element composition of Tagish Lake with other primitive carbonaceous chondrites. *Meteoritics & Planetary Science* 37:677–686.
Friend P., Hezel D. C., Barrat J.-A., Zipfel J., Palme H., and Metzler K. 2018. Composition, petrology, and chondrule-matrix complementarity of he recently discovered Jbilet Winselwan CM2 chondrite. *Meteoritics & Planetary Science*. https://doi.org/10.1111/maps.13139.
Fujiya W., Sugiura N., Hotta H., Ichimura K., and Sano Y. 2012. Evidence for the late formation of hydrous asteroids from young meteoritic carbonates. *Nature Communications* 3:627.
Garenne A., Beck P., Montes-Hernandez G., Chirac R., Toche F., Quirico E., Bonal L., and Schmitt B. 2014. The abundance and stability of "water" in type 1 and 2 carbonaceous chondrites (CI, CM and CR). *Geochimica et Cosmochimica Acta* 137:93–112.
Gibson E. K. Jr. and Bogard D. D. 1978. Chemical alterations of the Holbrook chondrite resulting from terrestrial weathering. *Meteoritics* 13:277–289.
Göpel C., Birck J.-L., Galy A., Barrat J.-A., and Zanda B. 2015. Mn-Cr systematics in primitive meteorites: Insights from mineral separation and partial dissolution. *Geochimica et Cosmochimica Acta* 156:1–24.
Grady M. M., Verchovsky A. B., Franchi I. A., Wright I. P., and Pillinger C. T. 2002. Light element geochemistry of the Tagish Lake CI2 chondrite: Comparison with CI1 and CM2 meteorites. *Meteoritics & Planetary Science* 37:713–735.
Grady M. M., Abernethy F. A. J., Verchovsky A. B., King A. J., Schofield P. F., and Russell S. S. 2014. The Jbilet Winselwan carbonaceous chondrite 2. Light element geochemistry: Strengthening the link between CM and CO meteorites? (abstract #5377). *Meteoritics & Planetary Science* 49.
Haack H., Grau T., Bischoff A., Horstmann M., Wasson J., Sørensen A., Laubenstein M., Ott U., Palme H., Gellissen M., Greenwood R. C., Pearson V. K., Franchi I. A., Gabelica Z., and Schmitt-Kopplin P. 2012. Maribo—A new CM fall from Denmark. *Meteoritics & Planetary Science* 47:30–50.
Hanowski N. P. and Brearley A. J. 2000. Iron-rich aureoles in the CM carbonaceous chondrites Murray, Murchison, and Allan Hills 81002: Evidence for in-situ aqueous alteration. *Meteoritics & Planetary Science* 35:1291–1308.
Hanowski N. P. and Brearley A. J. 2001. Aqueous alteration of chondrules in the CM carbonaceous chondrite Allan Hills 81002: Implications for parent body alteration. *Geochimica et Cosmochimica Acta* 65:495–518.
Hewins R. H., Bourot-Denise M., Zanda B., Leroux H., Barrat J.-A., Humayun M., Göpel C., Greenwood R. C., Franchi I. A., Pont S., Lorand J.-P., Cournède C., Gattacceca J., Rochette P., Kuga M., Marrocchi Y., and Marty B. 2014. The Paris meteorite, the least altered CM chondrite so far. *Geochimica et Cosmochimica Acta* 124:190–222.
Hezel D. C., Schlüter J., Kallweit H., Jull A. J. T., Al Fakeer O. Y., Al Shamsi M., and Strekopytov S. 2011. Meteorites from the United Arab Emirates: Description, weathering, and terrestrial ages. *Meteoritics & Planetary Science* 46:327–336.
Hiroi T., Peters C. M., Zolensky M. E., and Lipschutz M. E. 1993. Evidence of thermal metamorphism on C, G, B, and F asteroids. *Science* 261:1016–1018.
Hiroi T., Peters C. M., Zolensky M. E., and Lipschutz M. E. 1996. Thermal metamorphism of the C, G, B, and F asteroids seen from the 0.7-μm, 3-μm, and UV absorption strengths in comparison with carbonaceous chondrites. *Meteoritics & Planetary Science* 31:321–327.
Howard K. T., Benedix G. K., Bland P. A., and Cressey G. 2009. Modal mineralogy of CM2 chondrites by X-ray

diffraction (PSD-XRD). Part 1. Total phyllosilicate abundance and the degree of aqueous alteration. *Geochimica et Cosmochimica Acta* 73:4576–4589.

Howard K. T., Benedix G. K., Bland P. A., and Cressey G. 2010. Modal mineralogy of CV3 chondrites by X-ray diffraction (PSD-XRD). *Geochimica et Cosmochimica Acta* 74:5084–5097.

Howard K. T., Benedix G. K., Bland P. A., and Cressey G. 2011. Modal mineralogy of CM2 chondrites by X-ray diffraction (PSD-XRD). Part 2. Degree, nature and settings of aqueous alteration. *Geochimica et Cosmochimica Acta* 75:2735–2751.

Howard K. T., Alexander C. M. O'D., Schrader D. L., and Dyl K. A. 2015. Classification of hydrous meteorites (CR, CM and C2 ungrouped) by phyllosilicate fraction: PSD-XRD modal mineralogy and planetesimal environments. *Geochimica et Cosmochimica Acta* 149:206–222.

Kallemeyn G. W. and Wasson J. T. 1981. The compositional classification of chondrites I. The carbonaceous chondrite groups. *Geochimica et Cosmochimica Acta* 45:1217–1230.

King A. J., Schofield P. F., Howard K. T., and Russell S. S. 2015a. Modal mineralogy of CI and CI-like chondrites by X-ray diffraction. *Geochimica et Cosmochimica Acta* 165:148–160.

King A. J., Solomon J. R., Schofield P. F., and Russell S. S. 2015b. Characterising the CI and CI-like carbonaceous chondrites using thermogravimetric analysis and infrared spectroscopy. *Earth, Planets and Space* 67:198.

King A. J., Schofield P. F., and Russell S. S. 2015c. Thermal alteration of CI and CM chondrites: Mineralogical changes and metamorphic temperatures (abstract #5212). *Meteoritics & Planetary Science* 50.

King A. J., Schofield P. F., and Russell S. S. 2017. Type 1 aqueous alteration in CM carbonaceous chondrites: Implications for the evolution of water-rich asteroids. *Meteoritics & Planetary Science* 52:1197–1215.

Landsman Z. A., Licandro J., Campins H., Ziffer J., de Prá M., and Cruikshank D. P. 2016. The Veritas and Themis asteroid families: 5–14 μm spectra with the Spitzer Space Telescope. *Icarus* 269:62–74.

Lazzaro D., Angeli C. A., Carvano J. M., Mothé-Diniz T., Duffard R., and Florczak M. 2004. S^3OS^2: The visible spectroscopic survey of 820 asteroids. *Icarus* 172:179–220.

Lee M. R. and Nicholson K. 2009. Ca-carbonate in the Orgueil (CI) carbonaceous chondrite: Mineralogy, microstructure and implications for parent body history. *Earth and Planetary Science Letters* 280:268–275.

Lee M. R., Lindgren P., and Sofe M. R. 2014. Aragonite, breunnerite, calcite and dolomite in the CM carbonaceous chondrites: High fidelity recorders of progressive parent body aqueous alteration. *Geochimica et Cosmochimica Acta* 144:126–156.

Lee M. R., Lindgren P., King A. J., Greenwood R. C., Franchi I. A., and Sparkes R. 2016. Elephant Moraine 96029, a very mildly aqueously altered and heated CM carbonaceous chondrite: Implications for the drivers of parent body processing. *Geochimica et Cosmochimica Acta* 187:237–259.

Lindgren P., Lee M. R., Starkey N. A., and Franchi I. A. 2017. Fluid evolution in CM carbonaceous chondrites tracked through the oxygen isotopic compositions of carbonates. *Geochimica et Cosmochimica Acta* 204:240–251.

Lunning N. G., Corrigan C. M., McSween H. Y. Jr., Tenner T. J., Kita N. T., and Bodnar R. J. 2016. CV and CM chondrite impact melts. *Geochimica et Cosmochimica Acta* 189:338–358.

Marrocchi Y., Gounelle M., Blanchard I., Caste F., and Kearsley A. 2014. The Paris CM chondrite: Secondary minerals and asteroidal processing. *Meteoritics & Planetary Science* 49:1232–1249.

McAdam M. M., Sunshine J. M., Howard K. T., and McCoy T. M. 2015. Aqueous alteration on asteroids: Linking the mineralogy and spectroscopy of CM and CI chondrites. *Icarus* 245:320–332.

McCord T. B., Li L.-Y., Combe J.-P., McSween H. Y., Jaumann R., Reddy V., Tosi F., Williams D. A., Blewett D. T., Turrini D., Palomba E., Pieters C. M., De Sanctis M. C., Ammannito E., Capria M. T., Le Corre L., Longobardo A., Nathues A., Mittlefehldt D. W., Schröder S. E., Hiesinger H., Beck A. W., Capaccioni F., Carsenty U., Keller H. U., Denevi D. W., Sunshine J. M., Raymond C. A., and Russell C. T. 2012. Dark material on Vesta from the infall of carbonaceous volatile-rich material. *Nature* 491:83–86.

McPherson G. J., Bar-Matthews M., Tanaka T., Olsen E., and Grossman L. 1983. Refractory inclusions in the Murchison meteorite. *Geochimica et Cosmochimica Acta* 47:823–839.

McSween H. Y. Jr. 1979. Alteration in CM carbonaceous chondrites inferred from modal and chemical variations in matrix. *Geochimica et Cosmochimica Acta* 43:1761–1770.

Meier M. M. M., Grimm S., Maden C., and Busemann H. 2016. Do we have meteorites from the Veritas asteroid break-up event 8 Ma ago? (abstract #6291). *Meteoritics & Planetary Science* 51.

Mittlefehldt D. W. and Wetherill G. W. 1979. Rb-Sr studies of CI and CM chondrites. *Geochimica et Cosmochimica Acta* 43:201–206.

Miyamoto M. 1991. Thermal metamorphism of CI and CM carbonaceous chondrites: An internal heating model. *Meteoritics* 26:111–115.

Mortimer J., Verchovsky A. B., and Anand M. 2016. Predominantly non-solar origin of nitrogen in lunar soils. *Geochimica et Cosmochimica Acta* 193:36–53.

Nagao K., Inoue K., and Ogata K. 1984. Primordial rare gases in the Belgica 7904 (C2) carbonaceous chondrite. *Memoirs of National Institute of Polar Research Special Issue* 35:257–266.

Nakamura T. 2005. Post-hydration thermal metamorphism of carbonaceous chondrites. *Journal of Mineralogical & Petrological Sciences* 100:260–272.

Nakamura T. 2006. Yamato 793321 CM chondrite: Dehydrated regolith material of a hydrous asteroid. *Earth and Planetary Science Letters* 242:26–38.

Nakamura T., Nagao K., Metzler K., and Takaoka N. 1999. Heterogeneous distribution of solar and cosmogenic noble gases in CM chondrites and implications for the formation of CM parent bodies. *Geochimica et Cosmochimica Acta* 63:257–273.

Nakamura T., Kitajima F., and Takaoka N. 2000. Thermal effects on mineralogy, noble-gas composition, and carbonaceous material in CM chondrites (abstract). In *Workshop on extra-terrestrial materials from cold and hot deserts*, edited by Schultz L., Franchi I., Reid A., and Zolensky M. E. LPI Contribution 997. Houston, Texas: Lunar and Planetary Institute. pp. 61–63.

Nakamura T., Iwata T., Kitasato K., Abe M., Osawa T., Matsuoka M., Nakauchi Y., Arai Y., Komatsu M., Hiroi

T., Imae N., Yamaguchi A., and Kojima H. 2014. Reflectance spectra measurement of hydrated and dehydrated carbonaceous chondrites using the Near Infrared Spectrometer on Hayabusa 2 spacecraft (abstract #315). 37th Symposium on Antarctic Meteorites.

Nakato A., Nakamura T., Kitajima F., and Noguchi T. 2008. Evaluation of dehydration mechanism during heating of hydrous asteroids based on mineralogical and chemical analysis of naturally and experimentally heated CM chondrites. *Earth, Planets and Space* 60:855–864.

Nesvorný D., Bottke W. F., Levison H. F., and Dones L. 2003. Recent origin of the solar system dust bands. *The Astrophysical Journal* 591:486–497.

Nozaki W., Nakamura T., and Noguchi T. 2006. Bulk mineralogical changes of hydrous micrometeorites during heating in the upper atmosphere at temperatures below 1000°C. *Meteoritics & Planetary Science* 41:1095–1114.

Palguta J., Schubert G., and Travis B. J. 2010. Fluid flow and chemical alteration in carbonaceous chondrite parent bodies. *Earth and Planetary Science Letters* 296:235–243.

Pernet-Fisher J. F., Howarth G. H., Barry P. H., Bodnar R. J., and Taylor L. A. 2014. The extent of aqueous alteration within the Jbilet Winselwan CM2 chondrite (abstract #2386). 45th Lunar and Planetary Science Conference. CD-ROM.

Rodriguez-Navarro C., Ruiz-Agudo E., Rodriguez-Navarro A. B., and Ortega-Huertas M. 2009. Thermal decomposition of calcite: Mechanisms of formation and textural evolution of CaO nanocrystals. *American Mineralogist* 94:578–593.

Rubin A. E. 2007. Petrography of refractory inclusions in CM2.6 QUE97990 and the origin of melilite-free spinel inclusions in CM chondrites. *Meteoritics & Planetary Science* 42:1711–1729.

Rubin A. E. 2012. Collisional facilitation of aqueous alteration in CM and CV carbonaceous chondrites. *Geochimica et Cosmochimica Acta* 90:181–194.

Rubin A. E. 2015. An American on Paris: Extent of aqueous alteration of a CM chondrite and the petrography of its refractory and amoeboid olivine inclusions. *Meteoritics & Planetary Science* 50:1595–1612.

Rubin A. E., Trigo-Rodriguez J. M., Huber H., and Wasson J. T. 2007. Progressive aqueous alteration of CM carbonaceous chondrites. *Geochimica et Cosmochimica Acta* 71:2361–2382.

Russell S. S., King A. J., Schofield P. F., Verchovsky A. B., Abernethy F., and Grady M. M. 2014. The Jbilet Winselwan carbonaceous chondrite 1. Mineralogy and petrology: Strengthening the link between CM and CO meteorites? (abstract #5253). *Meteoritics & Planetary Science* 49.

Ruzicka A., Grossman J., Bouvier A., Herd C. D. K., and Agee C. B. 2015. The Meteoritical Bulletin, No. 102. *Meteoritics & Planetary Science* 50:1662.

Scott E. R. D., Keil K., and Stöffler D. 1992. Shock metamorphism of carbonaceous chondrites. *Geochimica et Cosmochimica Acta* 56:4281–4293.

Simon S. B., Davis A. M., and Grossman L. 1996. A unique ultrarefractory inclusion from the Murchison meteorite. *Meteoritics & Planetary Science* 31:106–115.

Simon S. B., Grossman L., Hutcheon I. D., Phinney D. L., Weber P. K., and Fallon S. J. 2006. Formation of spinel-, hibonite-rich inclusions found in CM2 carbonaceous chondrites. *American Mineralogist* 91:1675–1687.

Stelzner T., Heide K., Bischoff A., Weber D., Scherer P., Schultz L., Happel M., Schrön W., Neupert U., Michel R., Clayton R. N., Mayeda T. K., Bonani G., Haidas I., Ivy-Ochs S., and Suter M. 1999. An interdisciplinary study of weathering effects in ordinary chondrites from the Acfer region, Algeria. *Meteoritics & Planetary Science* 34:787–794.

Strekopytov S. V. and Dubinin A. V. 1997. Determination of Zr, Hf, Mo, W, and Th in standard reference samples of ocean sediments by inductively coupled plasma mass spectrometry. *Journal of Analytical Chemistry* 52:1171–1174.

Takenouchi A., Zolensky M. E., Nishiizumi K., Caffee M., Velbel M. A., Ross K., Zolensky A., Le L., Imae N., Yamaguchi A., and Mikouchi T. 2014. On the relationship between cosmic-ray exposure ages and petrography of CM chondrites (abstract #1827). 45th Lunar and Planetary Science Conference. CD-ROM.

Thangjam G., Nathues A., Mengel K., Schäfer M., Hoffmann M., Cloutis E. A., Mann P., Müller C., Platz T., and Schäfer T. 2016. Three-dimensional spectral analysis of compositional heterogeneity at Arruntia crater on (4) Vesta using Dawn FC. *Icarus* 267:344–363.

Tomeoka K. and Buseck P. R. 1985. Indicators of aqueous alteration in CM carbonaceous chondrites: Microtextures of a layered mineral containing Fe, S, O and Ni. *Geochimica et Cosmochimica Acta* 49:2149–2163.

Tonui E. K., Zolensky M. E., Hiroi T., Nakamura T., Lipschutz M. E., Wang M.-S., and Okudaira K. 2014. Petrographic, chemical and spectroscopic evidence for thermal metamorphism of carbonaceous chondrites I: CI and CM chondrites. *Geochimica et Cosmochimica Acta* 126:284–306.

Van Kooten E. M. M. E., Wielandt D., Schillar M., Nagashima K., Thomen A., Larsen K. K., Olsen M. B., Nordlund A., Krot A. N., and Bizzaro M. 2016. Isotopic evidence for primordial molecular cloud material in metal-rich carbonaceous chondrites. *Proceedings of the National Academy of Sciences* 113:2011–2016.

Velbel M. A. 2014. Terrestrial weathering of ordinary chondrites in nature and continuing during laboratory storage and processing: Review and implications for Hayabusa sample integrity. *Meteoritics & Planetary Science* 49:154–171.

Velbel M. A., Tonui E. K., and Zolensky M. E. 2012. Replacement of olivine by serpentine in the carbonaceous chondrite Nogoya (CM2). *Geochimica et Cosmochimica Acta* 87:117–135.

Velbel M. A., Tonui E. K., and Zolensky M. E. 2015. Replacement of olivine by serpentine in the Queen Alexandra Range 93005 carbonaceous chondrite (CM2): Reactant-product compositional relations, and isovolumetric constraints on reaction stoichiometry and elemental mobility during aqueous alteration. *Geochimica et Cosmochimica Acta* 148:402–425.

Vilas F. 2008. Spectral characteristics of Hayabusa 2 near-Earth asteroid targets 162173 1999 JU3 and 2001 QC34. *The Astronomical Journal* 135:1101–1105.

Wang M.-S. and Lipschutz M. E. 1998. Thermally metamorphosed carbonaceous chondrites from data for thermally mobile trace elements. *Meteoritics & Planetary Science* 33:1297–1302.

Weber H. W. and Schultz L. 1991. Noble gases in eight unusual carbonaceous chondrites (abstract #406). *Meteoritics* 26.

Wolf D. and Palme H. 2001. The solar system abundances of phosphorus and titanium and the nebular volatility of phosphorus. *Meteoritics & Planetary Science* 36:559–571.

Yabuta H., Alexander C. M. O'D., Fogel M. L., Kilcoyne A. L. D., and Cody G. D. 2010. A molecular and isotopic study of the macromolecular organic matter of the ungrouped C2 WIS 91600 and its relationship to Tagish Lake and PCA 91008. *Meteoritics & Planetary Science* 45:1446–1460.

Zolensky M. E., Bourcier W. L., and Gooding J. L. 1989. Aqueous alteration on the hydrous asteroids: Results of EQ3/6 computer simulations. *Icarus* 78:411–425.

Zolensky M. E., Barrett R., and Browning L. 1993. Mineralogy and composition of matrix and chondrule rims in carbonaceous chondrites. *Geochimica et Cosmochimica Acta* 57:3123–3148.

Zolensky M. E., Mittlefehldt D. W., Lipschutz M. E., Wang M.-S., Clayton R. N., Mayeda T. K., Grady M. M., Pillinger C., and Barber D. 1997. CM chondrites exhibit the complete petrologic range from type 2 to 1. *Geochimica et Cosmochimica Acta* 61:5099–5115.

Zolensky M. E., Mikouchi T., Hagiya K., Ohsumi K., Komatsu M., Chan Q. H. S., Le L., Kring D., Cato M., Fagan A. L., Gross J., Tanaka A., Takegawa D., Hoshikawa T., Yoshida T., and Sawa N. 2016. Unique view of C asteroid regolith from the Jbilet Winselwan CM chondrite (abstract #2148). 47th Lunar and Planetary Science Conference. CD-ROM.